JGP Journal of General Physiology

REVIEW

Allosteric coupling of RyR calcium channels: Is it relevant to the [patho]physiology of heart and muscle?

Eduardo Rios[1]

An examination of the phenomenon of coupled gating between ryanodine receptors, the Ca^{2+} channels of the sarcoplasmic reticulum of skeletal and cardiac muscle, essential for the execution of contraction upon electrical excitation. It asks whether the phenomenon—pairs of channels or larger groups, reconstituted in bilayers, opening and closing together—reflects allosteric interactions that require contact between channels, and whether the phenomenon occurs *in vivo* with sufficient prevalence to be relevant to physiology and pathophysiology. The examination covers definitions, observations of coupled currents, structural studies of channels, in purified or in native membranes, and quantitative modeling of the phenomena. It concludes with a negative answer to the question whether a physiological role is proven, but a hopeful perspective on further research.

Man does not realize how that which varies is a unity. There is a harmony of opposite tensions as there is one of bow and lyre.
-Heraclitus the Obscure.
(Epigraph in the article that first proposed allosteric effects: Changeux, 1961).

Some scientific questions have a way of entering and leaving the collective concerns of a research field, to then come back. One of these is the role, in cardiac and skeletal muscle physiology, of the intriguing "coupled gating" phenomenon exhibited by RyRs, Ca^{2+} release channels of the sarcoplasmic reticulum (SR) reconstituted in bilayers, first demonstrated for skeletal muscle channels by Andrew Marks and colleagues (Marx et al., 1998). Here, I review the topic, asking specifically *whether there are robust demonstrations of relevance of the molecular phenomenon*.

More specifically, I examine inter-RyR allostery, a term considered fully in the next section, used here to name cooperative phenomena (say, channel opening) induced mutually via a conformational mechanism that requires physical contact. This definition separates allostery from the cooperative channel opening that results from RyR activation by Ca^{2+}—the basis of the cell-level calcium-induced calcium release phenomenon (CICR; reviews by Endo [2009]; Ríos [2018]) and its paradigm, the Ca^{2+} spark (Cheng et al., 1993).

The opening of these channels (RyR1 in skeletal and RyR2 in cardiac muscle) allows Ca^{2+} to exit the SR and activate the mechanochemical processes of muscle contraction. The on-and-off engagement of the excitation–contraction (EC) coupling community with allosteric interactions between RyRs is justified by their potential roles in physiology and disease. The interactions were initially suggested by the structural evidence of interchannel contact in the orderly arrays (Franzini-Armstrong and Nunzi, 1983) of skeletal muscle junctions between the transverse (T) tubules and the SR. There, allosteric inducement was seen (and still is) as one of perhaps just two plausible mechanisms to activate RyR channels devoid of contacts with voltage-sensing channels of the T tubules (described with Fig. 4, below).

In spite of this head start in skeletal muscle, inter-RyR allosteric effects were quantitatively modeled first (Stern et al., 1999) as a device to offset the self-sustaining tendency of Ca^{2+} sparks of cardiac muscle, so they would robustly terminate. Because allostery can potentially synchronize channel opening and closing, it has been envisioned as a way to organize and discipline the operation of channel groups (say, both generation and taming of Ca^{2+} sparks; e.g., Sobie et al., 2002; Groff and Smith, 2008). In turn, this coordination by allostery is seen as providing a hub for modulation by ligands acting at RyR–RyR interfaces. Specifically, the immunophilins FKBP12 and FKBP12.6 have been proposed for the role (Marx et al., 2000); various defects in this modulation have been associated with cardiac disease (Wehrens et al., 2003; Lehnart et al., 2008) and elicited work aimed at disease remediation in cardiac and

[1]Department of Physiology and Biophysics, Section of Cellular Signaling, Rush University, Chicago, IL, USA.

Correspondence to Eduardo Rios: eduardo_rios@rush.edu.

skeletal muscle (Wehrens et al., 2004, 2005; Bellinger et al., 2009). Allosteric interactions between RyR1 have also been envisioned, informally as yet, for activation of the "orphan" RyR1, channels devoid of voltage sensors in the "skipping" pattern of connections of the skeletal muscle T-SR junctions (Block et al., 1988) illustrated with Fig. 4.

But, does reality agree with the many expectations and hypotheses? How good is the evidence that inter-RyR allostery and its malfunction are actually behind this rich phenomenology? This is the single concern and justification for the article.

For readers interested solely in the bottom line, my answer to the focal question is no—inter-RyR allostery is a fact, but *its relevance for function has not been demonstrated*. What makes reading on worthwhile is the narrative of the collective work that backs this answer, plus all the qualifications and recent developments that enrich the conclusion, to one of *continued belief in the reality and relevance of the mechanism*. Keeping these apparently disjointed statements in mind will help one appreciate and enjoy all the work that is in-between.

This examination is organized in six sections: "Allosteric and allostery," a brief review of the origins and meaning of the terms; "The currents," where the coupled gating data are reviewed; "The channels," with attention to structure and spatial contacts of individual RyRs and their arrays; "The models," where the theoretical and computational approaches to these phenomena are discussed; and "Conclusions" and "Perspectives," where I tried to summarize what is known, together with suggesting possible approaches that might improve this knowledge. Text boxes provide detail on quantitative approaches.

Given the wide range of work, and perhaps inspired by the channels' interactions, I undertook this meta-analysis in a gregarious, cluster-of-scientists mode. For that, I collected opinions, references, illustrations, even unpublished work, from many colleagues, who uniformly kindly and unguardedly responded to my questions. The harvest was rich. I will quote some of their opinions with attribution; others will be left uncredited, but it should be clear that the article draws freely from the intelligence and productivity of many researchers.

This article does not intend to be an exhaustive review; it will inevitably omit valuable work. Besides, I delved into subjects outside my experience. Therefore, the conclusions will be tentative and open-ended. I welcome corrections, objections, disagreements, additions, or any other comments. I suggest *JGP* Letters to the Editor as an avenue.

Allosteric and allostery

The most authorized and entertaining account of these terms' inception is in Changeux (2011), where J.-P. Changeux credits it to his doctoral mentors Jacques Monod and Francois Jacob, in the discussion of his presentation to a Cold Spring Harbor Symposium (Changeux, 1961). The term was proposed to qualify the inhibition of the *entry* enzyme in a bacterial synthetic chain by the *final* product, very different from its first substrate, hence unlikely to be acting on the same site. Allosteric (another site) was proposed as the logical alternative to the well-known mechanism of enzyme feedback by its substrate or analog molecules. In that same terrific discussion, Bernard Davis reflected on the similarity of the allosteric regulation with the properties of the binding of O_2 to hemoglobin, which alters positively the affinity for the next O_2 molecule. Davis's comment incorporated positive feedback to the mix, stressed a similarly virtuous outcome (maintain a metabolite in a narrow concentration range in the negative feedback case, narrow the concentration swing needed for the effect—binding O_2—in the other), and planted the seed for the "MWC" quantitative model (Monod et al., 1965) that justified, together with enzyme control, the relationship between O_2 concentration and saturation of hemoglobin.

A more restrictive meaning of allosteric is in the requirements for the "allosteric proteins" to which the MWC model applies. These must be oligomeric, with at least one dyad axis of symmetry (one about which a 180° rotation produces an identical structure). Valuable tools for our task emerge from these precedents: individual RyRs are formed by four identical protomers in a closed ring; they therefore satisfy the MWC conditions. Not unexpectedly, the depolarization-induced opening of RyR1s follows quantitatively the predictions of the MWC model if the voltage-sensing Ca_Vs of the nearby T tubules take the place of the allosteric ligands (Ríos et al., 1993). The present article, however, deals with interactions *between* RyR tetramers; as we shall see, those between RyR1s follow the MWC requisites, but the cardiac RyR2s' apparently do not. In a look back at MWC after 50 years, Changeux (2012) concludes that the MWC conditions for allostery are sufficient (the property was found in every allosteric protein where it was sought) but not necessary. Thus, to encompass a wider range of phenomena, this article gives allosteric its less restrictive meaning: a conformational interaction with consequences for gating, away from the gated pore.

The currents

Allosteric interactions between ion channels of diverse sorts have been documented and/or hypothesized to explain their function (Duke and Bray, 1999; Duke et al., 2001; Molina et al., 2006; Naundorf et al., 2006; Dekker and Yellen, 2006; Dixon et al., 2022; Navedo et al., 2010; rev. by Bray and Duke [2004]). The examination here will be limited to interactions between RyR1 isoforms and between RyR2 isoforms.

Coupled gating refers to a phenomenon first demonstrated by Marx et al. (1998) for recombinant rabbit RyR1 expressed in and purified from sf9 cells, observations rapidly repeated in native RyR2 channels, purified from dog hearts (Marx et al., 2001). Common aspects of the phenomenon seen in both studies are in Fig. 1, in panels reproduced from Fig. 2 of Marx et al. (2001). While bilayer reconstitution with microsomes or liposomes and either isoform results more often than not in the incorporation to the bilayer of multiple channels (M. Fill, personal communication), about 10% of the multichannel sets exhibit coupled gating of a pair, while trios are seen in ∼1% of cases in the experience of these authors.

Coupled gating was observed systematically and frequently enough to quantify its features in only a few laboratories, while

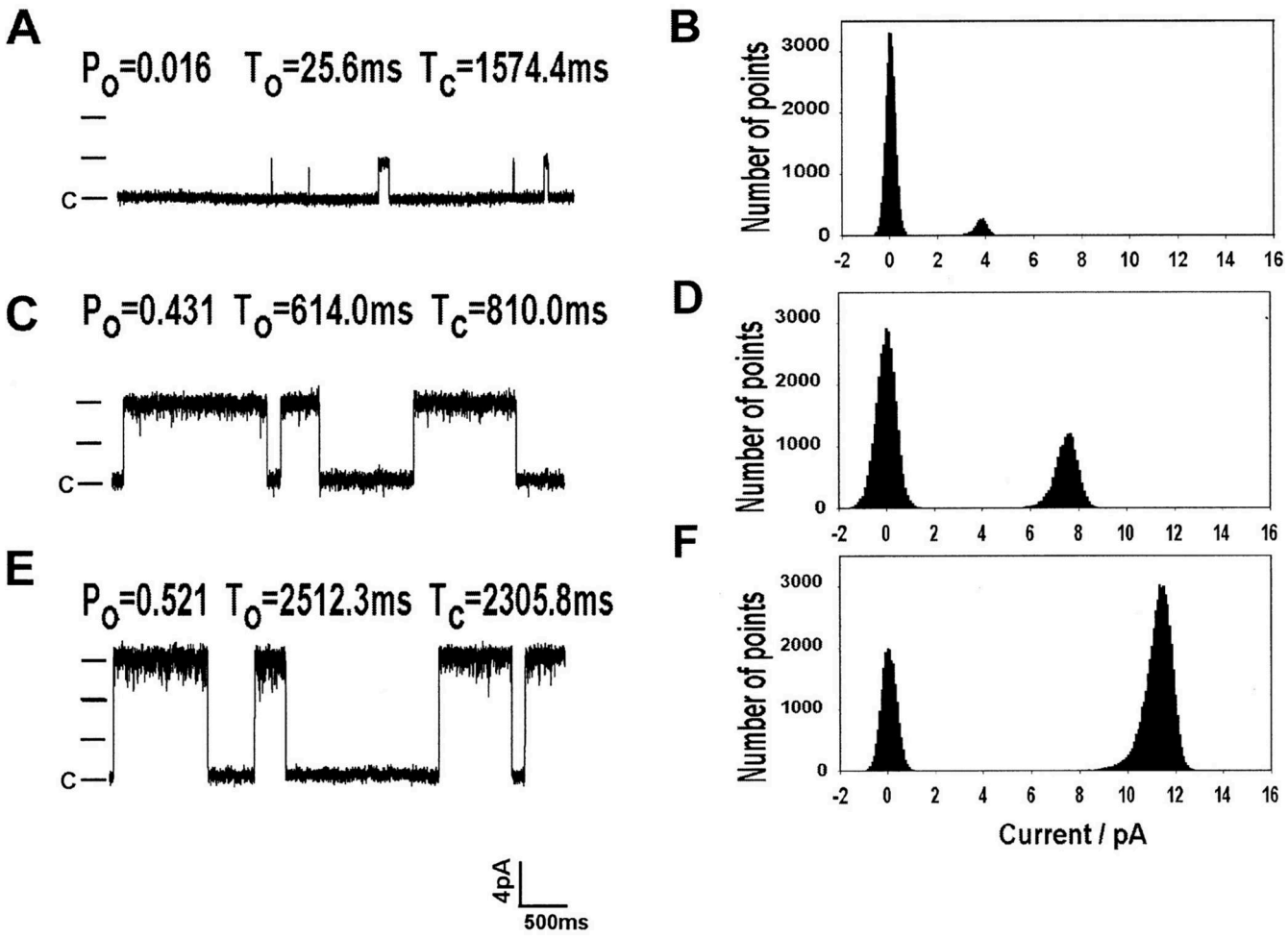

Figure 1. **First report of coupled gating between RyR2 channels.** Dog cardiac microsomes reconstituted in bilayers. **(A and B)** Ca^{2+} current (flowing from a *trans* chamber compartment—the SR-luminal side of the channels—with ~50 mM free $[Ca^{2+}]$, to a *cis* compartment with physiological cytosolic $[Ca^{2+}]$) through an individual channel, with an all-points current histogram in B, consistent with a single channel current of 4 pA. **(C and D)**, Currents of 8 pA and histogram suggest a pair of coupled channels. **(E and F)** Currents and histogram consistent with a trio of fully coupled channels. Note the absence in D and F of any peak for individual openings, and in the 12-pA peak in F a skew, with a "tail" toward lower values that suggests partial closings. Figure minimally modified from Fig. 2 of Marx et al. (2001), reproduced by courtesy of Andrew Marks. Fig. 1 is reprinted with permission from Circulation Research.

many other groups—I am told—observed the behavior only occasionally. Fig. 2, reprinting Fig. 2 in the data-rich report of Gaburjaková and Gaburjaková (2010), illustrates the dependence of coupled gating of native rat RyR2 on cytosolic $[Ca^{2+}]$. As the study demonstrates with robust statistics, this Ca^{2+} dependence is similar to that of channels gating independently. To complete this sampling of classic datasets, Fig. 3 (reproducing Fig. 3 in Porta et al. [2012]) illustrates coupled gating of RyR1s from rabbit skeletal muscle.

These three examples have in common currents through two or more channels that are not gating independently. In all three, the channels are passing current from *trans* to *cis*, i.e., in the normal direction of physiological Ca^{2+} release (as reconstitution is rigged so that the SR = luminal side of the channels faces the *trans* side of the bilayer). The current is driven by the difference between a $[Ca^{2+}]_{trans}$ of ~50 mM (a concentration grossly greater than the physiological $[Ca^{2+}]_{SR}$ of 1 mM or less) and a $[Ca^{2+}]_{cis}$ near the physiological range for the cytosol.

The phenomena depicted in the three illustrations have substantial differences. Gating of two or three cardiac channels in Fig. 1, C and E, is perfectly coupled; channels *always* gate together, as ascertained by the lack of intermediate peaks in the all-points histograms in Fig. 1, D and F. Full coupling with these characteristics was also visible in the records of currents through RyR1 channels in the 1998 report of Marx et al. In contrast, the records of current through coupled cardiac channels in Fig. 2 (Gaburjaková and Gaburjaková, 2010) show frequent flickering to states *OC* (or *CO*) from *OO*. The difference with the records in Fig. 1 is not attributable to composition of solutions or electronic filtering. Marta Gaburjaková suggested species difference (rat in her study vs. dog in the other) as an explanation. It could also be due to lower pass filtering in the experiments of Fig. 1, as bilayer chambers with larger apertures were used there (again, information from M. Gaburjaková). The differences are yet greater with the currents through RyR1 channels in Fig. 3 (Porta et al., 2012). These are currents through multiple channels, which may engage in coupled gating

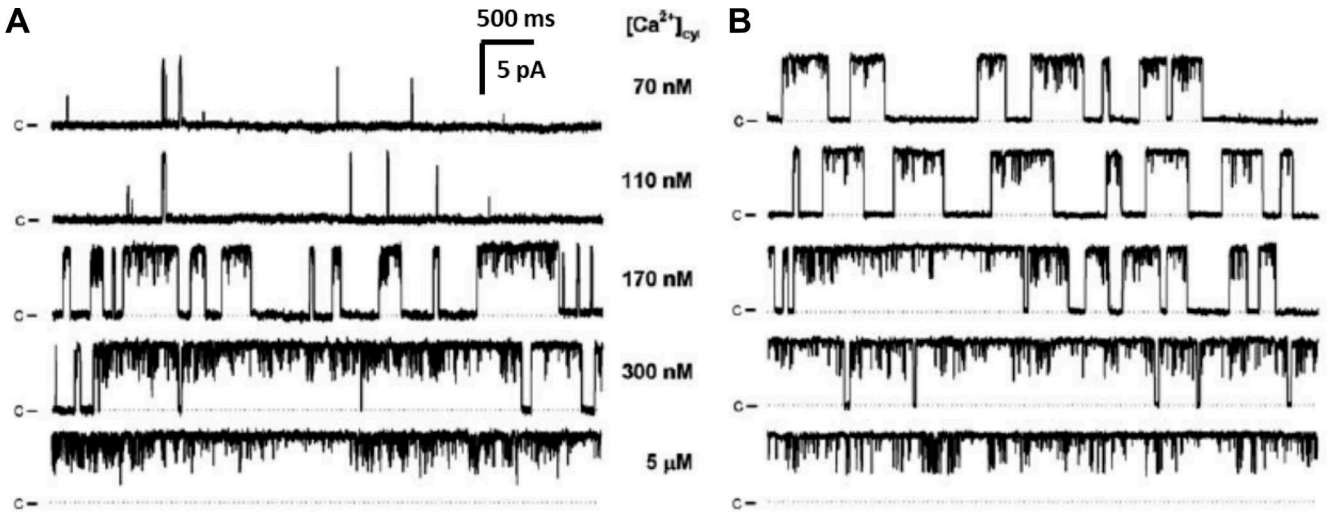

Figure 2. **RyR2 channels gating together retain their sensitivity to Ca^{2+}.** Rat cardiac microsomes reconstituted in bilayers. Ca^{2+} currents flowing from *trans* to *cis* driven by a similar $[Ca^{2+}]_{trans}$ as in Fig. 1. **(A and B)** Panels A and B show currents from channels in a low-activity and a high-activity category, respectively, differing in P_{open} at physiological $[Ca^{2+}]_{cis}$ by more than an order of magnitude. The activation by $[Ca^{2+}]_{cis}$ has similar half-effect concentrations and maximal activations in both categories, also similar to those found with independently gating channels. Note here clear transitions to the *CO/OC* configuration, frequent starting from *OO* but essentially absent starting from *CC*. Figure minimally modified from Fig. 2 of Gaburjaková and Gaburjaková (2010), reproduced by courtesy of Marta and Jana Gaburjaková. Fig. 2 is reprinted with permission from Springer Nature.

intermittently, usually by pairs (as in Fig. 3 B) but sometimes in greater synchronous groupings (Fig. 3 C).

The detailed analysis from J. Copello's lab (see also Box 1) revealed a complexity that was not present in the earlier results (Marx et al., 1998; Marx et al., 2001; Ondrias and Mojzisová, 2002; Gaburjaková and Gaburjaková, 2010), including bilayer reconstitutions resulting in a mix of channels in which some were seen to gate independently while others gated concertedly, partially or fully coupled.

Do these engrossing phenomena have any claim to being physiological? The $[Ca^{2+}]_{trans}$ in these classic examples is far from it. The closest the experiments with Ca^{2+} currents have come to the ≤1 mM physiological luminal range is 5 mM (Gaburjaková and Gaburjaková, 2010); at this $[Ca^{2+}]$, the currents had similar properties to those recorded at higher concentrations. From the existing evidence (which includes structural data discussed later), a tentative conclusion is that the phenomenon can occur at physiological concentrations, not just in bilayers but also *in vivo*. Also suggestive of physiological operation is the demonstration by Porta et al. (2012) that coupled gating requires the presence of ATP and Mg^{2+} at physiological concentrations in the cytosolic (*cis*) solution (or what was thought to be physiological, now revised down for cardiac ATP: (Eisner and Murphy, 2024; Rhana et al., 2024). A caveat remains, revisited with the Models section: the variety of coupled gating modes noted in the previous comparison, together with their scarcity, suggests that some of the observed interactions may not occur *in vivo* often enough to be relevant.

What is the mechanism of coupled gating? Two RyRs passing Ca^{2+} from lumen to cytosol next to each other will inevitably experience mutual influences due to their penchant for activation by Ca^{2+} (a.k.a. CICR) and perhaps Ca^{2+}-dependent inactivation. A fast Ca^{2+}-activated opening of "channel #2" after "#1" could look like allosterically coupled gating of the pair. How to tell one from the other? A demonstration of coupled gating with currents carried by CICR-disabling Ba^{2+} is the gold standard. The original description of the phenomenon with RyR1 (Marx et al., 1998) included the statement that the phenomenon was observed with Ba^{2+} as carrier, but no data were presented. Coupled RyR2 current with Ba^{2+} as carrier was reported for two channels in Marx et al. (2001), but the most robust evidence is in Gaburjaková and Gaburjaková (2010), where permeation of Ca^{2+} and Ba^{2+} is demonstrated in detail. Differences in gating kinetics of individual vs. coupled channels, described in the same article, are reasonably taken as additional evidence of allosteric coupling.

While the existence of the coupled gating phenomenon seems indisputable, the initial excitement that drove many labs to its study waned years later because of the difficulty to elicit it with sufficient frequency, and because, in the view of many, it could not be reliably distinguished from a form of CICR. Its occurrence with Ba^{2+} has been especially difficult to reproduce (M. Fill, personal communication); its presence with physiological $[Ca^{2+}]_{lumen}$ was only observed with Cs^{+} currents, and in that case convincingly demonstrated to be mediated by CICR (Laver et al., 2004). Adding to the skepticism, Alexandra Zahradníková disputed the relevance of this coupling, based on the ability of models that assume allosterically independent RyRs to explain quantal properties and other aspects of Ca^{2+} sparks in cardiac muscle (Zahradníková et al., 2010).

In my view, the robust demonstration of coupled Ba^{2+} currents through cardiac channels (Gaburjaková and Gaburjaková, 2010), and the apparent independence of the phenomenon from luminal-to-cytosolic Ca^{2+} flow (seen with RyR1 by J. Copello's

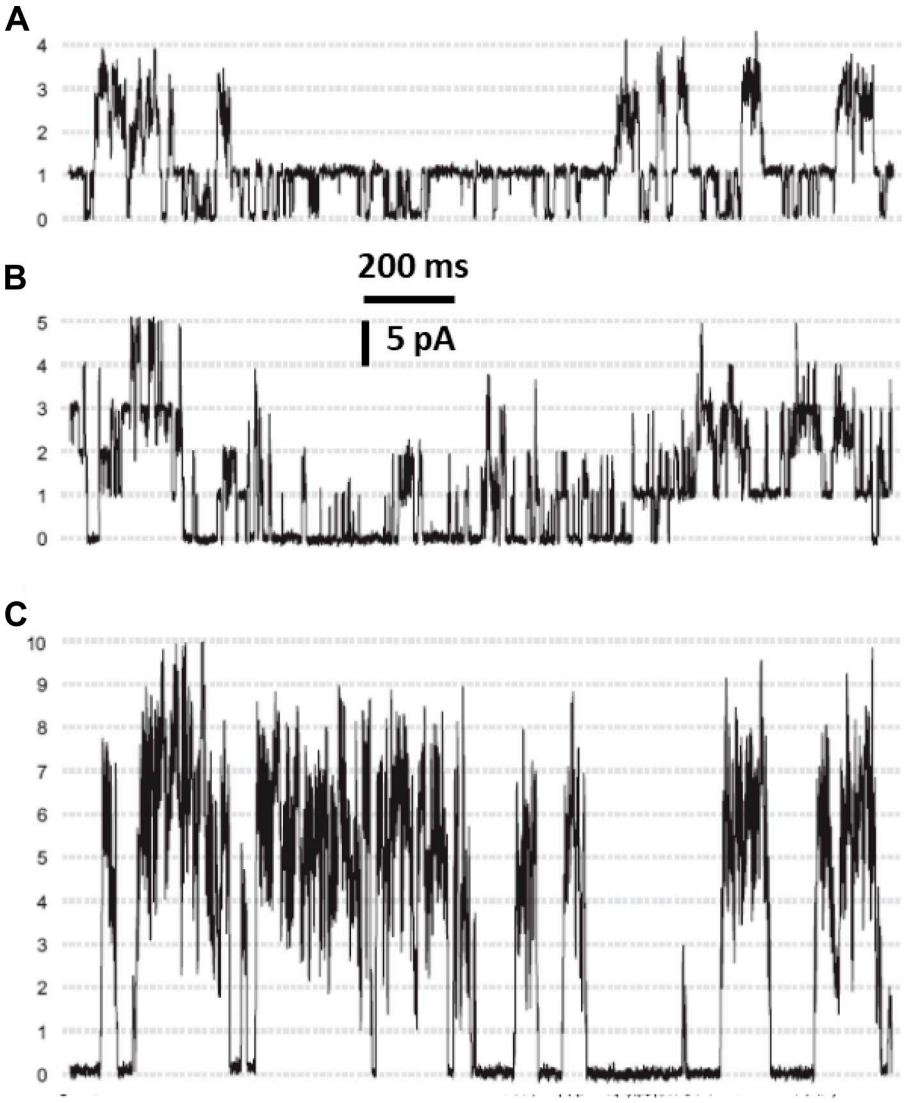

Figure 3. **RyR1 channels show partial coupling.** Reconstituted microsomes from rabbit skeletal muscle, passing Ca^{2+} current, as in Figs. 1 and 2, from a *trans* compartment with ~50 mM free [Ca^{2+}]. Unlike the previous examples, these authors report a requirement for Mg^{2+} and ATP at physiological concentrations in the *cis* compartment for the occurrence of coupled gating. **(A)** As interpreted by the authors, one channel gates independently and three others join in synchrony. **(B)** Two independently gating channels are intermittently joined by two pairs of coupled RyRs independent of each other, contributing individual currents of ~5 pA. **(C)** Authors identify 10 levels of current, from "fully coupled" channels, which in their terminology means that no channel is gating independently, but coupling is not complete or obligatory, as revealed by a *CR* measure (Box 1) different from 0. Fig. 3 of Porta et al. (2012) reproduced by courtesy of Julio Copello. Fig. 3 is reprinted with permission from American Physiological Society.

team, personal communication) are sufficient evidence of the allosteric, Ca^{2+}-independent nature of the coupling interaction. That the phenomenon is difficult to demonstrate, and that models can ignore it and still reproduce observations *in situ* can be evidence of irrelevance but not of nonexistence. The balance of the evidence shows that inter-RyR allostery is real.

FKBPs raise the stakes

The excitement caused by the initial descriptions of the phenomenon was enhanced by tantalizing observations of effects of the immunophilins FKBP12 and FKBP12.6, small peptidyl-prolyl isomerases that are targets of the immunosuppressants FK506 (Liu et al., 1991) and rapamycin (Brown et al., 1994). Both FKBP12

Box 1. **Cooperativity ratio**

Establishing actual coupled gating requires some work, as two independent channels can gate synchronously now and then, just by chance. When coupling is partial, as in Fig. 3, its presence is established by measures of the separation between the actual distribution of open states and the binomial distribution of N identical channels gating independently with individual probability p:

$$P(m \text{ open}) = \frac{N!}{m!(N-m)!} p^m (1-p)^{N-m} \quad (1)$$

Porta et al. (2012) use a "cooperativity ratio," *CR* (Krouse and Wine, 2001), justified in an Appendix of Porta et al. (2012), as a measure that emerges from the amplitude histograms.

$$CR \quad \frac{(k-1)}{2k} \frac{\Phi_1^{\,2}}{\Phi_0 \Phi_2} \quad (2)$$

where k is the maximum number of open channels in the record, and the Φs are the fractions of time at current levels indicated by the subindex. For the two-channel case, it can be easily verified, using Eq. 1, that *CR* equals 1 for identical independent channels, 0 in the fully coupled case (Fig. 1, simply because $\Phi_1 = 0$), and positive <1 in cases of partial gating (for these verifications, it is useful to remember that 0! = 1).

and FKBP12.6 bind stoichiometrically to the RyR1 tetramer (Jayaraman et al., 1992), but only FKBP12.6 binds with high affinity to the cardiac isoform (Timerman et al., 1996; Lam et al., 1995). Marx et al. (1998) reported that the addition of FKBP12 to the *cis* side of a bilayer chamber with recombinant RYR1 channels gating independently had the dual effect of removing subconductance states—an effect previously demonstrated by Brillantes et al. (1994)—and inducing coupled gating. Conversely, removal of the immunophilin by the addition of rapamycin uncouples channels functionally—although, these authors stated, the channels remained physically together (Marx et al., 1998).

FKBPs were found to be associated with the RyR1 early in the chronology of structural exploration, bound to a peripheral region of the tetramer (Wagenknecht et al., 1996; Samsó et al., 2009) later refined to a location counterclockwise from every corner, next to the tandem Repeat 12 and the SPRY domain cluster (refer to Fig. 5 for a summary of RyR structure). The location is similar for bound FKBP12.6 on RyR2, and is precisely within the region of intertetramer contact and overlap identified by Cabra et al. (2016). This border location is therefore consistent with the proposed involvement of the immunophilins in intertetramer allostery, as is their enzymatic activity, a chiral isomerization that can potentially cause significant conformational changes.

Substantial functional roles of FKBPs in skeletal muscle were demonstrated in the early 2000s by the groups of Robert Dirksen and Susan Hamilton. In "dyspedic" (RyR-lacking) myotubes, Avila et al. (2003) expressed RyR1 with a V-G replacement at position 2,461, a mutation that prevents binding of FKBP12 (Gaburjaková et al., 2001), and found a 50% reduction in Ca^{2+} release. The effect was firmly assigned to the missing immunophilin because the alternative V-I replacement (which by substituting an isoleucine transforms the local RyR1 sequence to that of RyR2) prevented the binding of FKBP12 but not that of coexpressed FKBP12.6, and the coexpression rescued the functional deficit. Tang et al. (2004) confirmed the effect on a mouse engineered for skeletal muscle-specific ablation of FKBP12, while also showing other deficiencies, in a complex phenotype. While Avila et al. argued for the loss of coupled channel opening as preferred mechanism of the EC coupling loss, the complexity of effects revealed by these early studies detracts from the value of FKBPs as tools to identify and evaluate allosteric coupling. FKBPs are definitely players of skeletal muscle EC coupling, but their role in allostery is difficult to isolate.

The focus on FKBPs increased as pathophysiological implications were proposed for their variable occupancy of the RyR tetramers (Marx et al., 2000). The proposal included that phosphorylation by PKA at serine 2808, enhanced in heart failure, caused dissociation of FKBP12.6 from RyR2, which resulted in appearance of substates, disappearance of coupled gating, and an overall increase in propensity of the channel to open (with consequences for increased Ca^{2+} leak from the SR and diastolic instability). Thus, the question of coupled gating and its functional implications became subsumed within the broader excitement, and later controversy on the roles of the immunophilins and phosphorylation. A summary of the controversy is in an editorial by Donald Bers (2012) for *Circulation Research*. Specifically, the "stabilizing" roles proposed for FKBPs were questioned by Xiao et al. (2007), who showed that neither the absence nor the removal of FKBP12.6 induced subconductance states or changed the activation properties of RyR2, effects also found to be absent when examining the consequences of FKBP suppression on spontaneous Ca^{2+} release in RyR2-expressing cultured cells. In agreement, Guo et al. (2010) found that just 10–20% of intact myocytes from rats and mice have a bound FKBP12.6, which, even accepting the "stabilization" role proposed, severely challenges the relevance of this protein to physiology and pathophysiology.

Considering the abundant but contradictory evidence, I conclude that the requirement of the immunophilins for coupled gating has not been demonstrated. This conclusion, however, does not exclude all relevance of these proteins to either function or spatial arrangement of RyR2s, as considered in the following section.

The channels

As written above, the initial enthusiasm for coupled gating ebbed circa 2012 due to the difficulties inherent to its study in bilayers and its overlap with the robust CICR mechanism. However, structural studies using selective crystallization, multiple avenues to super-resolution, and the paradigm-changing direct detection electron microscopy (with the near-atomic resolution that it provides and the resulting computational modeling that it enables) have come to the rescue. As outcomes, they elucidated the contacts between RyRs in ever-increasing detail and provided striking arguments for the existence of contact-mediated effects, thus renewing interest in inter-RyR allostery.

The skeletal muscle RyRs were studied first

The systematic contact between RyRs was first visualized in electron microscopic images of skeletal muscle (Franzini-Armstrong and Nunzi, 1983; Block et al., 1988), revealing "feet" (as the channel initial silhouettes were named) placed in two-row, two-dimensional paracrystalline arrays, which populated the SR sides of "triad" junctions where SR meets T tubules. This arrangement is illustrated in Fig. 4. The array of RyRs and voltage-sensing DHPRs in one T-SR junction was later proposed as a functional unit, the couplon (Stern et al., 1997). Additionally in cultured BC3H1 cells, in some types of muscle fibers, and in most fibers during differentiation, junctions are formed by association between wide SR cisternae and the surface plasmalemma (rather than T tubules); in them, feet are arranged in large plaques of multiple rows, with the same disposition and tilt angles of the adult. The ability to form these ordered arrays is an intrinsic property of RyR1, which does not depend on chaperones, a specific scaffold or a muscle context (reviewed by Yin et al. [2008]).

Progress continued with the goals of increased resolution and imaging *in situ* and in different functional situations, applying tools like single-particle EM of purified receptors (Samsó et al.,

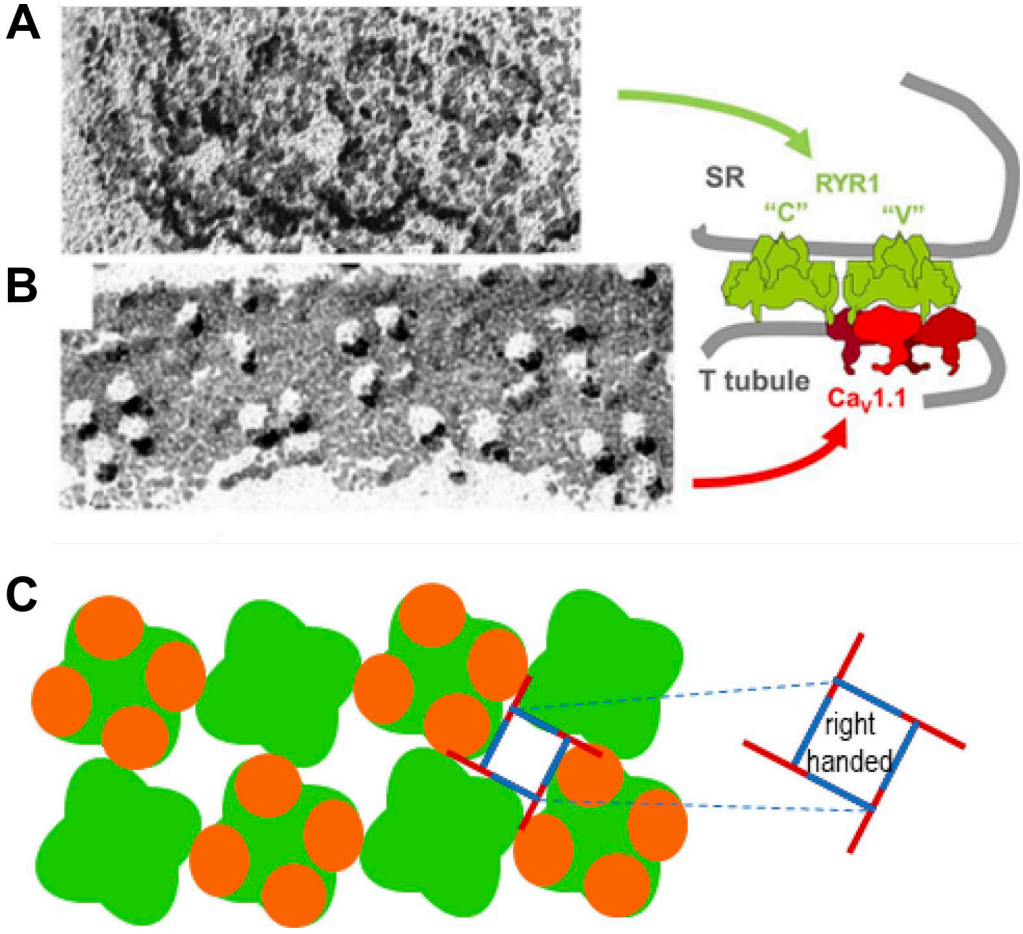

Figure 4. **Components of a junction between an SR terminal cisterna and a transverse (T) tubule. (A)** Freeze-dried junctional SR membrane from guinea pig showing RyR1 tetramers of ∼28-nm sides. **(B)** Tetrads of particles (Ca_Vs) in a freeze-fractured T tubule membrane from toadfish muscle, presented with the same orientation and magnification. **(C)** Canonical couplon in which every other channel is in contact with Ca_Vs (orange elements). The stoichiometric overlap of Ca_Vs and RyRs, first proposed by Block et al. (1988), was confirmed by direct observation by Xu et al. (2024); see Fig. 7 below. The diagram illustrates chirality or handedness, as viewed from outside the cell, in the way RyR tetramers make mutual contact. This orientation, conventionally called right-handed, has the intertetramer approaches occurring at the tetramers' edge, to the right-hand side of every corner. The contacts are said to be antiparallel, as the corners of the tetramers involved are on opposite ends of the contact segment. The overlapping Ca_Vs make the contact asymmetric, a feature relevant for the dynamics of the interactions. Relabeled Fig. 1 of Ríos et al. (2019), which includes images from Block et al. (1988).

2009), x-ray diffraction of crystals of domains or domain groups that yielded partial atomic structures (Yuchi et al., 2015; Amador et al., 2009; Tung et al., 2010), various approaches to imaging native muscles including EM tomography (Wagenknecht et al., 2015; Wagenknecht et al., 2002), and advances in direct detection cryo-EM tomography (Zalk et al., 2015; Yan et al., 2015; des Georges et al., 2016; Efremov et al., 2015).

RyR imaging provided evidence of allosteric control

Using the tools above, combined with well-planned choices of conditions for imaging, the structuralists were able to produce observations with mechanistic implications for gating. These purely structural studies with functional implications continue a long line of insightful imaging work, like the paradigmatic first report of the stoichiometric arrangement of RyRs and voltage sensors (Block et al., 1988; see Fig. 4), which supported the conformational control of the Ca^{2+} release channels at an early time. This early evidence was interpreted first as supporting the direct or "orthosteric" type of action of voltage sensors on RyRs implicit in the "toilet plunger" model of Chandler et al. (1976), which proposed a stopper of the channel pore with a rigid handle operated by T membrane voltage; but the consensus soon evolved to a subtler, allosteric connection between $Ca_V1.1$ sensors and RyR1 channels (Ríos et al., 1993; reviewed by Hernández-Ochoa and Schneider [2012]).

A significant contribution by structuralists in explicit support of inter-RyR allosteric coupling was the observation of a downward movement of the distal cytosolic RyR1 domains, likened to a swivel or flexion, away from the T membrane (Samsó et al., 2009; see also Efremov et al., 2015; Steele and Samsó, 2019), which results in a decrease by 1 nm or greater of their distance to the SR membrane. This movement, which occurs together with widening of the cytosolic vestibule (patent in the side view of Fig. 5) and opening of the

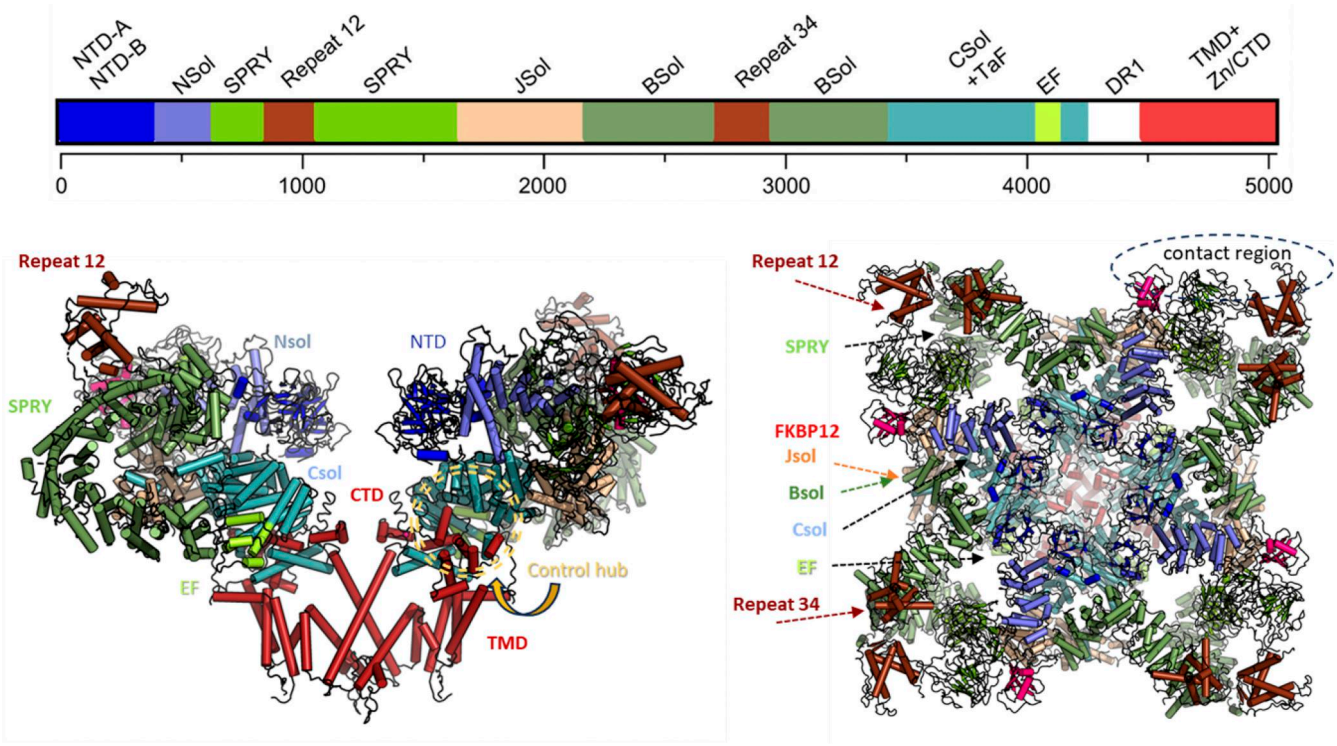

Figure 5. **Structure of RyR1.** The sequence map at top identifies domains and segments named following des Georges et al. (2016), in color code that is maintained in the diagrams and labels. The side view has two of the four protomers removed for clarity. The "top" or "*en-face*" view is as seen from the cytosolic side. The arrows on the *en-face* view are color-coded, except for three set in black for visibility. In the side view, the double-dash circle (indicated by a curved arrow) encloses the control hub that includes the binding sites of the three canonical agonists: Ca^{2+}, ATP, and caffeine. "Sol" stands for the multiple α-solenoid regions, regarded as a relatively inert, convoluted stem from which globular domains hang like fruits. NTD and CTD stand for N- and C-terminal domains, both of which line a central cytosolic-side vestibule. The large SPRY (SP1a kinase and ryanodine receptor) stretch is subdivided into three domains. The tandem Repeats 12 and 34 are also known as P1 and P2. While the diagrams represent RyR1, RyR2 is highly similar. The ellipse at top right in the *en-face* view marks the domains believed to participate in RyR2–RyR2 "oblique" contacts (cf. Fig. 8), namely, Repeat 12, SPRY1, and the associated protein FKBP12, which in RyR2 could be replaced by RyR12.6. They occupy approximately one third of the edge, leftward of every corner. The diagrams are a gift from Filip Van Petegem (University of British Columbia, Vancouver, Canada).

channel pore, could mediate coupled gating if coerced on a linked neighbor RyR1.

Additionally, FKBP12 was found to be associated with high occupancy in rabbit RyR1 under closed-state conditions (Steele and Samsó, 2019), a conformation in which the cytoplasmic RyR cap was at a "high," upward angle (i.e., toward the T membrane). In contrast, the FKBP12-bound RyR structure imaged under open-pore conditions had the characteristic downward flexion of the cytoplasmic cap, while the closed, FKBP12-free RyR ("apoRyR") showed an intermediate angle. Interpreting the flexion angle as a measure of the free energy of the channels, the observations suggest a greater energy difference between open and closed when the immunophilin is bound. The greater energy change could result in increased stability of the closed state. For this interpretation to hold, additional assumptions are needed, regarding, among others, the energy barriers opposing the transition. We get more deeply into the energetics of coupling in the Models section.

Suggestive observations relevant to allosteric coupling are illustrated in Fig. 6 (Chen and Kudryashev, 2020). They were made by averaging subsets ("subtomograms") of cryo-electron tomograms of rabbit muscle native membranes in the then thinnest-possible slices of frozen tissue, milled down to ~100 nm by a focused ion beam ("cryo-FIB," Marko et al., 2007; Wagenknecht et al., 2015). Most images show both leaflets of the SR membrane. As shown earlier by Renken et al. (2009) and Wagenknecht et al. (2015), the visible membrane exhibits curvature, downward concavity. As seen in Fig. 6 A, bottom, the curvature changes measurably with putative activation. Thus, on average in the apoRyR images the curvature was 1/(50 nm), while in the images of so-called ryRyR1 (obtained in the presence of Ca^{2+} and ryanodine, corresponding to an open pore in high-resolution images of des Georges et al., 2016), the curvature increased to 1/(35 nm). This observation made with purely structural approaches is yet another with potentially profound functional implications. Indeed, if channel opening associates with (or induces) a local increase in membrane curvature, and if this curvature does not change abruptly over short spaces, the increase will invade membrane under the nearby channels. There, a reciprocal effect, predictable by conservation of energy, should take place: the increased curvature should induce or facilitate channel opening. Such effect would thus provide an additional, unexpected allosteric coupling mechanism, favoring a spatial "contagion" of both open and closed states. The energetics

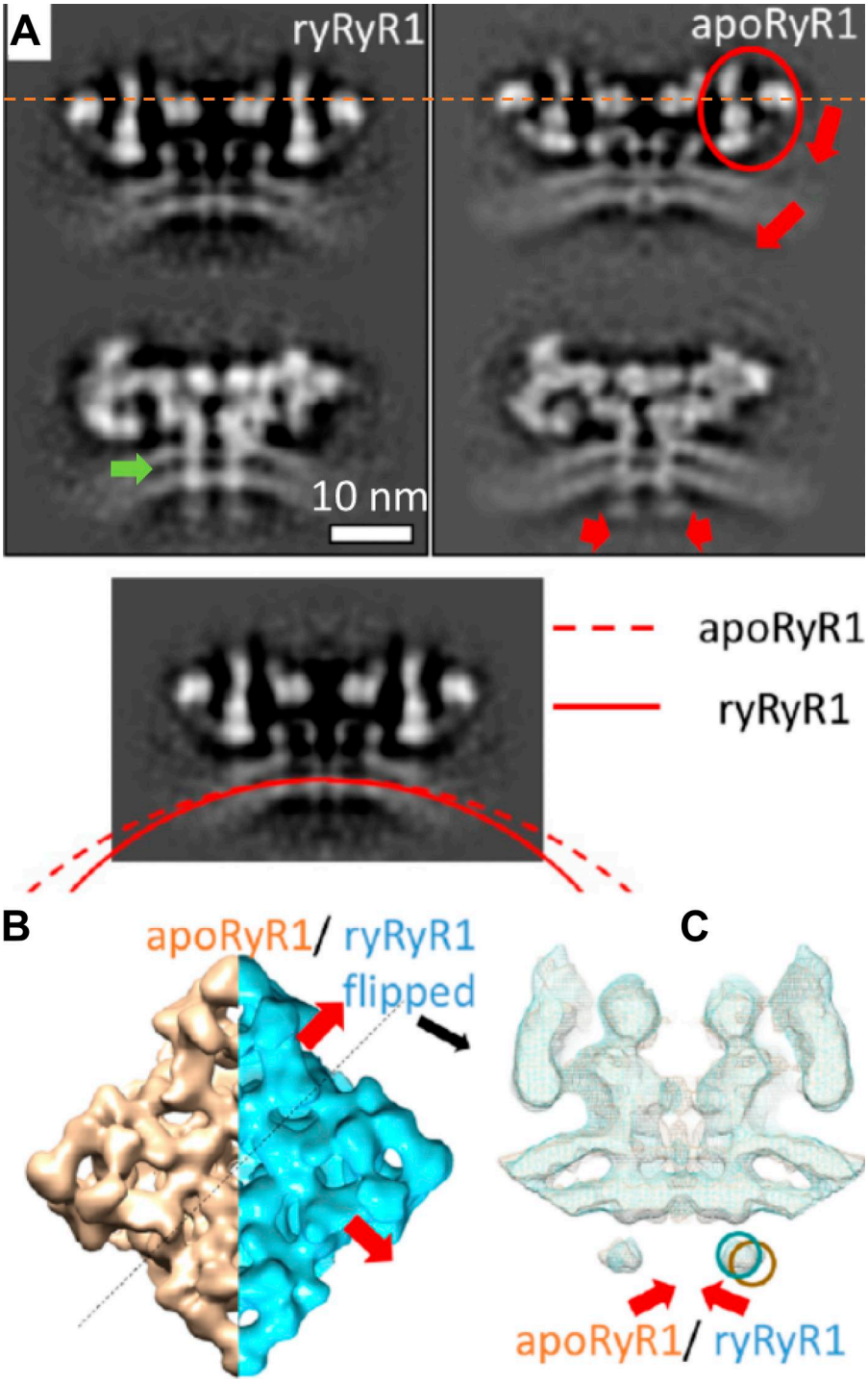

Figure 6. **RyR1–RyR1 structures in native membranes. (A)** RyR1 in TC-enriched SR fractions from rabbit muscle. Images, obtained from cryo-electron tomography and subtomogram averaging, reached a resolution of 17.5 Å. ryRyR1 names preparations in high Ca^{2+} and ryanodine, presumably an open channel configuration. Views are through the middle slice of the reconstruction (top panels) and at the level of intra-SR extensions (bottom panel). In the left panel, the outer domains in the mushroom cap are displaced downward from their positions in the closed structure (in red oval; movement also indicated by red arrows). In the lower panel, arcs in red trace the fitted curvatures of the SR membrane. **(B)** Rendering of apoRyR1 and ryRyR1 (mirror-flipped) viewed from the cytoplasm. Again, red arrows mark regions that move the most, in this case on the putatively open structure. **(C)** Section through the isosurface, with plane indicated by the dashed line in B. Red arrows indicate movement of the SR extensions (dark orange circle: apoRyR1; blue, ryRyR1). Extensions are visible also in-between the SR membrane leaflets (green arrow in A). Reproduced with minor modifications from Fig. 4 of Chen and Kudryashev (2020) by courtesy of Misha Kudryashev.

of this hypothetical, membrane-mediated allostery is considered in Box 2, in the next section.

Other notable observations in the study of Chen and Kudryashev (2020) include visualization of transmembrane densities that are distinct from the transmembrane "pore" domain, insensitive to the functional state and noticeable between the SR membrane leaflets (green arrow in Fig. 6 A). Also visible are intra-SR extensions that move toward the channel axis upon activation (movement indicated by short red arrows in panels A and C). The nature of these densities and extensions is unknown, but the authors ascribe them to transmembrane helices or helix bundles, assigned tentatively to stretches of the protein sequence not allocated to known domains in present RyR1 models. Goforth et al. (2003) discuss functional and structural changes due to interactions between transmembrane proteins and membrane lipids.

By averaging subtomograms that showed two tetramers in contact, and fitting a suitable atomic model, Chen and Kudryashev (2020) identified five stretches involved in the closest contacts. These are 15- to 25-residue-long helices located

Box 2. **Energetics of curvature change**

The strength of this possible and plausible coupling mechanism can be gauged, tentatively, from the energy change in the measured bending. Helfrich's equation (Helfrich, 1973) evaluates the bending energy of a homogeneously curved patch of membrane of area A as

$$(1/2)\, A\, \kappa\, (2H - H_0)^2 \qquad (3)$$

where κ is bending rigidity, and H and H_0 are the mean and spontaneous curvature, respectively (a term proportional to Gauss curvature that cancels in the differences is omitted). Assuming κ = 20 kT and H_0 = 0, the change from 1/35 to 1/50 nm^{-1} requires 14.2 kT per channel. (If instead one assumed that the spontaneous curvature is the one observed with closed channels, 1/50 nm^1, the result would be 12.5 kT).

A useful term for comparison is the energy associated with activation of one channel, presumably by the electrically driven movement of four voltage sensors. This energy can be roughly estimated under three assumptions: (1) all 4 DHPRs engaged by one RyR1 must move to cause it to open, (2) only one of the 4 voltage sensing domains in the DHPR pseudotetramer is involved, and (3), 2 charged residues in the moving S4 helix must traverse the membrane electric field in the process. Assumption (1) is arbitrary, unpublished work of my laboratory favors 3 sensors as a sufficient minimum, instead of 4. Assumptions (2) and (3) are informed by work of Bernhard Flucher's group (Pelizzari et al., 2024; Heiss et al., 2025). Under these assumptions, if 4×1×2 elementary charges undergo a 100 mV change, the energy input is 0.8 eV or 30 kT, not much greater than that required for the curvature change.

between residues 2950 and 3254, a region immediately C-terminal to Repeat 34 (also known as P2) in one of the α-solenoid regions near the center of the protein sequence (see map in Fig. 5).

This assignment of interacting stretches was largely confirmed by a study of Xu et al. (2024), who also applied the cryo-FIB method to visualize mouse triad junctions *in situ*. This study achieved multiple feats: it captured both Ca_V1 tetrads and RyR tetramers in their native membranes; it identified, averaged, and visualized Ca_V1-RyR1 "supercomplexes," and it imaged multichannel RyR arrays in the native SR membrane in near-native couplon formation.

Of the above, the most significant accomplishment is perhaps the imaging together and *in situ* of the complex constituted by the tetrad of DHPRs and the RyR. The contact of these essential couplon components had been assumed, based on a variety of evidence, for nearly 50 years (starting with the aforementioned "plunger" model of Chandler et al., 1976). The study by Xu et al. (2024) finally revealed the complexes for all to see, as well as their "skipping" pattern in the checkerboard array of RyRs. The work also started to unravel the structural details of the interaction and affirmed the allosteric properties of the RyR, with its ostentatious cytoplasmic cap as complex antenna for the reception of multiple signals.

For the purposes of the present article, Xu et al. (2024) achieved two relevant advances. They roughly confirmed the sites of inter-RyR contacts proposed by Chen and Kudryashev (2020), with details illustrated in Fig. 7: they also produced a coarse-grained molecular dynamics simulation of four RyR1 tetramers, which shows them converging spontaneously to a multimer with native checkerboard pattern (i.e., corner-to-corner, in the right-handed configuration diagrammed in Fig. 4).

This convergence does not just confirm the intrinsic tendency of RyRs to adopt their trademark pattern but contributes separate evidence of allosteric gating, as the tendency to the native assemblage was found more consistently when the simulation was done with tetramers in the open configuration. This component of the study can be questioned for starting at relatively short intertetramer distances, and with relatively low angles between tetramers. Less biased starting points, however, would demand a too costly extension of the simulation times, as candidly disclosed to me by the authors. In spite of these qualms, the observation not only supports allosteric gating but also provides a definite indication that allostery operates by favoring the open state (key to The Models, below). (Xu et al. [2024] conclude that "...the activated RyR1 then activates the neighboring RyR1s instantly,...through physical coupling." Based on other evidence and arguments developed in the present article, I disagree with the certainty in that conclusion).

RyR2 poses additional possibilities and unknowns

RyR2 is highly homologous with RyR1, with overall sequence similarity of 80–85%. RyRs share overall dimensions and domain structure (e.g., Peng et al., 2016), but in contrast to the strict checkerboard arrangement of junctional RyR1s, RyR2s appear in a variety of groupings. They are present within three structures: peripheral couplings with the plasma membrane, dyad junctions with transverse tubules, and corbular SR, not associated with exterior membranes (Franzini-Armstrong et al., 1999). Key to the issue of allosteric interaction, these RyR2 clusters are seen to contain more units than the RyR1 couplons, but are less compact, and a regular skeletal muscle-like arrangement of RyR2 has never been visualized (Hayashi et al., 2009; Baddeley et al., 2009; Asghari et al., 2014). Additionally, RyR2 has a higher sensitivity to activation by Ca^{2+} (Murayama and Kurebayashi, 2011), which enables the essential role of CICR in contractile activation of cardiac muscle. This propensity for activation by Ca^{2+} constitutes a first obstacle to the identification of cardiac channel cooperativity based on allosteric interactions, rather than mediated by Ca^{2+}.

Substantial progress regarding RyR2 grouping is credited to the laboratories of Montserrat Samsó and Edwin Moore. Exploiting the natural tendency of purified RyRs to aggregate, Cabra et al. (2016) examined EM images of spontaneously paired RyR2s from pig heart. Fig. 8 A shows averages of five classes of pairs, aligned on one of the components, prepared in high Ca^{2+}. The varying blur in the component not used for alignment defines the flexibility of the interaction. By comparison with images of preparations in low Ca^{2+}, not shown here, high Ca^{2+} does not seem to introduce major changes, an observation that differs from the effects found by Xu et al. (2024) in their MD simulations of RyR1. The oblique configurations are so named because the orientations of the partners differ by 12°—another remarkable difference with the pairings of RyR1. The oblique-rigid motif

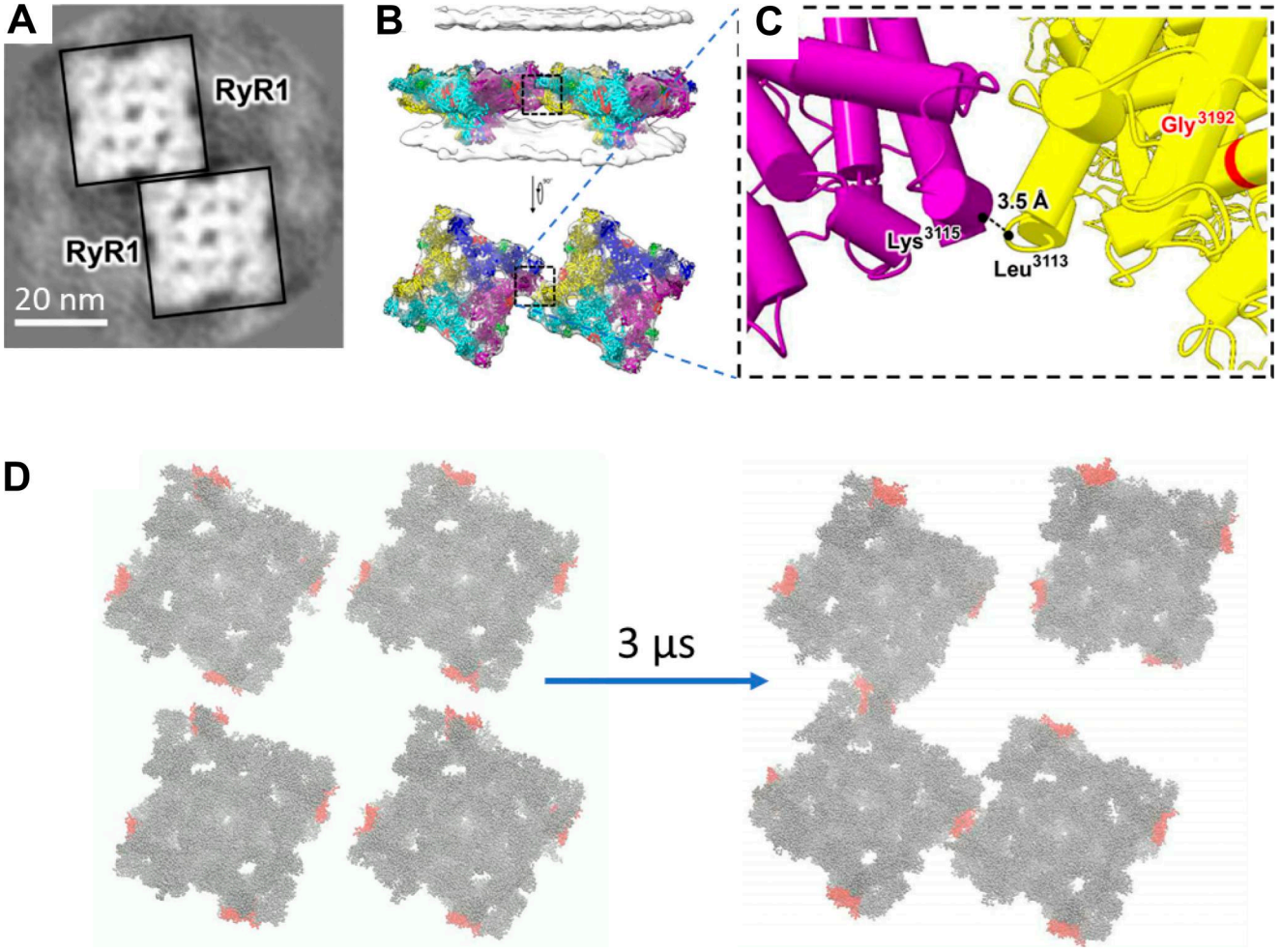

Figure 7. **Self-organizing of RyR1 in native membranes. (A)** Slice of an average of subtomograms showing paired tetramers in ultrathin frozen lamellae of rat skeletal muscle. Scale bar, 20 nm. **(B)** Averaged map of dimeric RyR1 tetramers *in situ*, showing both T tubule and SR membrane. A near-atomic model of RyR1-FKBP12 is fitted into the map. **(C)** Enlargement of the contact site in panel E, with nearest residues Lys^{3115} and Leu^{3113} indicated. Gly^{3192}, in red, is a reported site for a mutation associated with premature death in two patients. **(D)** Initial and near-final frames of a trajectory movie of a coarse-grained MD simulation of RyR1s in the open state. Residues ranging from 2951 to 3240 are shown in red. Note that the contact sites are located immediately to the right of every corner, in contrast to the "left-handedness" of RyR2–RyR2 contacts noted with Figs. 5 and 8. Images are reproduced with minimal annotation changes in panels from Fig. 3 and frames from Supplemental Movie 4 in Xu et al. (2024). Shared by courtesy of Guohui Li, Yun Zhu, and Fei Sun. Fig. 7 is reprinted with permission from The American Association for the Advancement of Science.

(Fig. 8 A) is most interesting because of the substantial overlap of the component image contours, about 20 nm^2, which tells of an intimate interaction conducive to allostery. As noted for RyR1, the handedness of the RyR2 averages in the pair was always the same (albeit left-handed), and the interactions were again antiparallel.

As done with RyR1, Cabra et al. (2016) modeled the rigid interactions of RyR2 by overlaying a near-atomic structure of RyR1 (not a typo). The adjoining pairing (Fig. 8 A) put in contact bulky groups that seem unlikely to establish energetically favorable interactions. Most interesting were the correspondences in the oblique pairing, with a detail in Fig. 8, C and D; the pairings involve Repeat 12 (a.k.a. P1, adjacent to the vertex), SPRY1, and, when present, bound FKBP12.6. In *en-face* views from the cytosol, these three groups occupy about one third of the tetramer's edge, counterclockwise from the vertex. Using exclusively this oblique pairing, Cabra et al. were able to arrange clusters of tetramers in rows of alternate orientation (Fig. 8 E), which overlapped with arrays described in muscle of scorpions (Loesser et al., 1992).

If this "oblique–rigid" interaction occurred frequently *in vivo*, it could constitute a basis for inter-RyR allostery. However, and unlike the native inter-RyR1 contacts in the skeletal muscle couplon, this dimer does not satisfy the MWC requisite symmetry (invariance on a 180° rotation). As stated by Changeux (2012), this is not a fatal impediment, but it adds to the odds against a relevant allosteric interaction between cardiac RyRs.

The advances with purified receptors were matched well by studies *in situ*. EM tomography in rat hearts, single cardiomyocytes, and human ventricle tissue showed variegated arrangements, going from arrays to smaller and disordered groupings and to isolated tetramers (Asghari et al., 2014). These distributions were altered by conditions of preparation, including $[Mg^{2+}]$ and phosphorylation. Fig. 9 shows selected

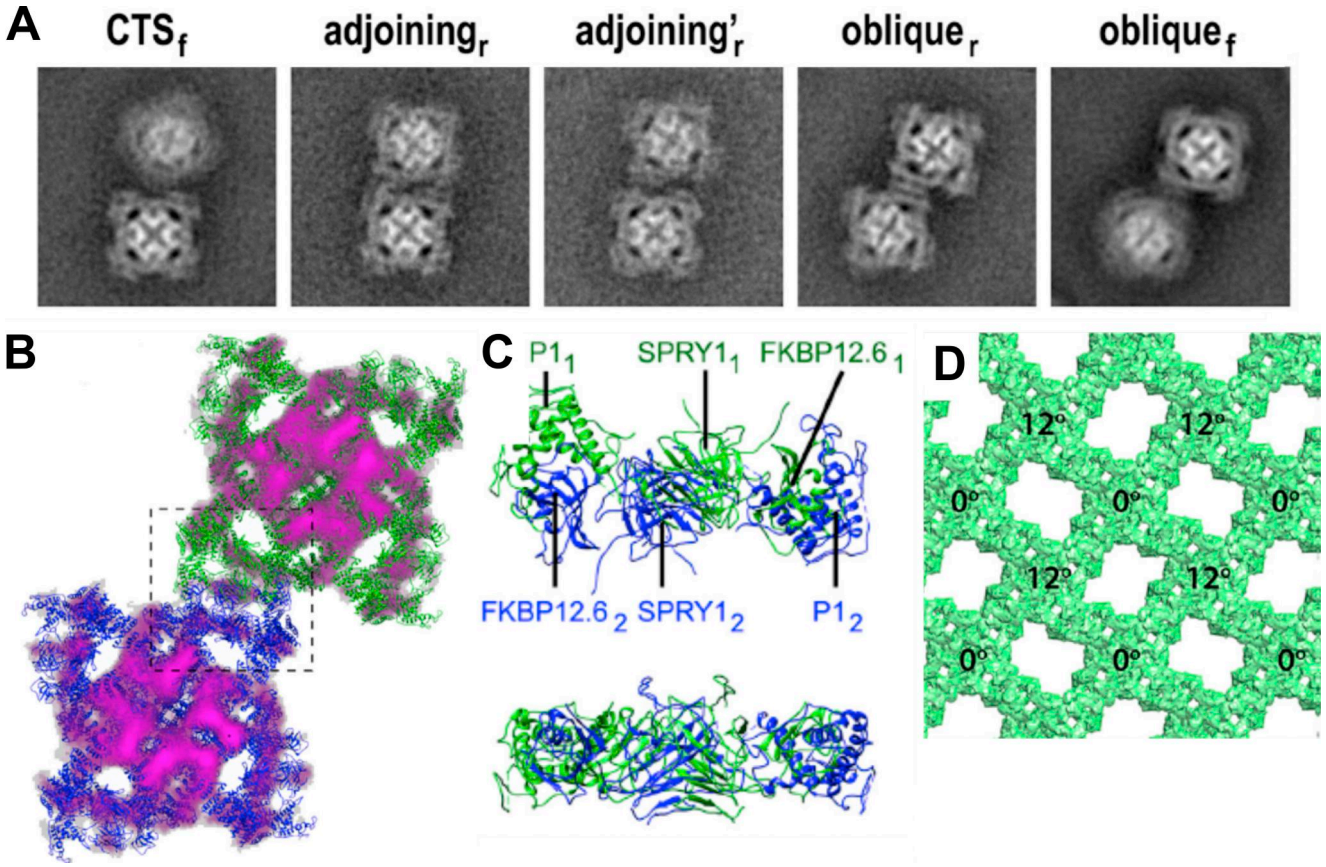

Figure 8. **Pairwise contacts of cardiac RyRs.** Transmission electron microscopy averages of RyR2 from pigs' hearts, purified, incubated in 100 µM Ca^{2+}, and negatively stained. **(A)** Averages of contacting pairs (selected by techniques that exclude chance proximity), classified in five groups and aligned on one member. CTS—center to side. The subindex (f or r) distinguishes a rigid and a flexible association mode, the latter evident in the fuzziness of the nonaligned member of the pair. **(B)** Near-atomic model of the oblique interaction (structure includes FKBP12). Note that in this view from the cytosolic side, the interaction RyR2–RyR2 is left-handed (compare with RyR1–RyR1 interactions in Fig. 4 and 7). **(C and D)** Enlargement of the boxed region in B, indicating the antiparallel contacts between domains P1 (or Repeat 12), SPRY1, and FKBP12. **(E)** Diagram of a hypothetical array, built exclusively on the basis of the oblique interaction, which requires alternation between rows with mutual tilts of 12°. Panels from Fig. 2 and 4 in Cabra et al. (2016), reproduced by courtesy of Montserrat Samsó. Fig. 8 is reprinted with permission from Elsevier.

frames from videos that visualize reconstructions of rat cardiomyocyte dyads from tomograms (Asghari et al., 2020). Backed by robust statistics, the images illustrate the main outcomes of the study, as follows: interactions of RyR2 clusters are indeed diverse, and mutable in response to external agents. Mutual positions range from proximity to a variety of contacts, including pairings described as "side-by-side" (similar to the "adjoining" category of Cabra et al., 2016) and "array-like" (roughly consistent with Cabra's "oblique," "corner-to-corner," and "corner-to-side" categories). Fig. 9 A shows a dyad with what the authors call "model" RyRs (i.e., reconstructed from tomograms). The corresponding histogram of nearest-neighbor distances, shown in the original figures, features two peaks, at 28 and 34 nm, corresponding, respectively, to side-to-side and array-like pairings. Exposure to saturating FKBP12.6 put most pairwise interactions in the side-to-side category (Fig. 9 B), while a phosphorylation cocktail turned most into array-like pairings (Fig. 9, C and D).

In a tour de force, Asghari et al. (2020) managed to record Ca^{2+} sparks from individual clusters that they then fixed and imaged by electron tomography. They found that the sparks from FKBP12.6-saturated channels, predominantly in side-to-side interactions, had lower frequency than the untreated preparations, while phosphorylation increased their frequency by several-fold, as well as the spark signal mass. The effect of phosphorylation was greater in the presence of FKBP12.6 (Fig. 9 D), an observation contrary to the claim that phosphorylation removes the immunophilin from RyR2.

The studies with RyR2 offer a mixed bag of possibilities and problems for interchannel allostery. The loose groupings, together with the greater propensity of RyR2 for Ca^{2+}-mediated opening, favor coupling mechanisms based on activation by Ca^{2+}. On the other hand, RyR2 engages in intricate contact interactions, the topology of which changes in living cells together with the channels' proclivity to open, with exposure to the immunophilins and phosphorylation. That the effects of these agents include only minor shifts in cluster density does not support mediation by Ca^{2+} and favors instead an allosteric mechanism for the functional changes. However, the generally loose and variable aspect of the native clusters suggests that the

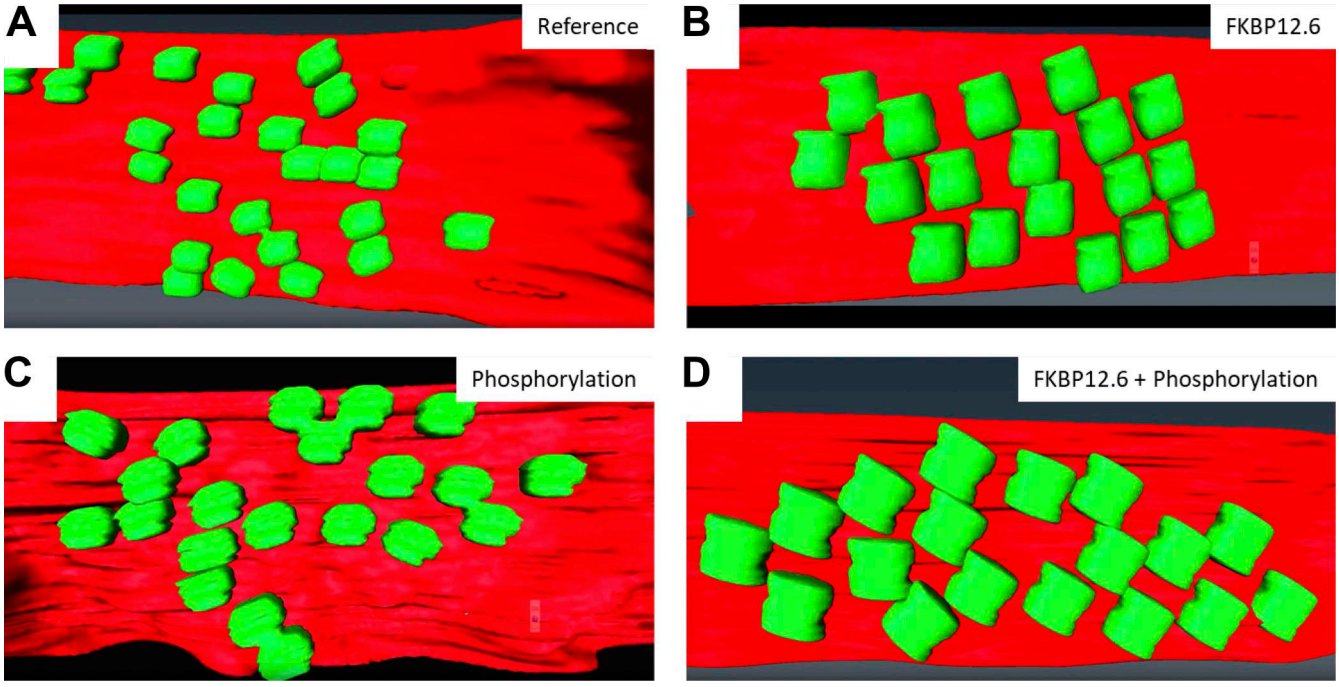

Figure 9. **Cardiac RyRs in their native membrane.** Selected frames from reconstructions of dyads and RyR tetramers derived from tomograms of rat ventricle. **(A)** Junctional SR membrane, representative of a resting myocyte, showing a variety of tetramer pairings. **(B)** Different junction, after exposure to saturating FKBP12.6. **(C)** After exposure to a phosphorylation cocktail. **(D)** Phosphorylation plus saturation with FKBP12.6. For a correlation with properties of Ca^{2+} sparks recorded before structural imaging in the same preparations, see text. Frames from videos 1, 4, 2, and 6, respectively, of Asghari et al. (2020), reproduced by courtesy of Edwin Moore.

role of allostery is minor, compared with the robust and well-understood gating actions of Ca^{2+}.

The models

The abundant literature of models of Ca^{2+} release from the SR attempts in skeletal muscle to reconstruct the cellular Ca^{2+} transient of EC coupling, while in cardiac muscle, it sets more numerous and bigger simulation tasks, ranging from the events in the single molecule to the electromechanics of the working heart in all its complexity. The discussion here will stay narrowly focused on gauging roles of allosteric coupling.

RyR–RyR interactions underlying Ca^{2+} sparks

Early modeling attempted to reproduce the charismatic Ca^{2+} spark phenomenon found in myocytes (Cheng et al., 1993; Tsugorka et al., 1995; Nelson et al., 1995), and the modeling continued more recently for neurons (Vierra et al., 2021). To grasp the difficulties found in the process, it seems fair to recognize that Ca^{2+} sparks, now seen as a paradigm of cooperative gating, had their multichannel origin established only after a laborious process (e.g., Klein et al., 1996; Cannell et al., 1995; Blatter et al., 1997; Jiang et al., 1999; Shirokova et al., 1996). Their cooperative nature was only settled by the demonstration (Ríos et al., 1999; Soeller and Cannell, 2002; Baylor, 2005) that they require Ca^{2+} fluxes much larger than what one RyR could provide (Mejía-Alvarez et al., 1999; Kettlun et al., 2003). This consensus opened the spigot for models of their mechanism.

Allostery in skeletal muscle couplons

The panorama of intermolecular allostery in skeletal muscle is rich and complex: physiologically, RyR1s are activated to open by an allosteric interaction with $Ca_V1.1$ (Rios and Brum, 1987; Tanabe et al., 1988; Nakai et al., 1996) and modulated and perhaps caused to close by calsequestrin (Canato et al., 2010; Sztretye et al., 2011). These interactions can be described as operating *along* the functional axis of the couplon, either in the forward direction (as depolarization-induced Ca^{2+} release) or retrogradely, in the effects of the presence of RyR1 on $Ca_V1.1$ gating, demonstrated by Nakai et al. (1996), and in the modulation of RyR1 gating by calsequestrin. In contrast to these robust *axial* effects, *transversal* inter-RyR1 allostery has not been invoked in gating models. In fact, the only quantitative proposals for mechanically transmitted inter-RyR effects that I know of are either to establish the skipping pattern of RyR-Ca_V1 contacts (Ríos et al., 2019) or to recruit the skipped RyRs in the checkerboard -- but invoking Ca^{2+}, rather than allostery as the final activator (Stephenson, 2024). As summary, I paraphrase an observation by Woll and Van Petegem (2022): it is surprising that inter-RyR1 allostery has been so difficult to demonstrate, and therefore absent from models, considering that this is the sole interaction that physically resists purification protocols, unlike other mechanical links known to affect gating. Later in this section, I will describe how the methods used to model inter-RyR2 allostery can be adapted to the more hopeful task of modeling allosteric interactions between RyR1s in the skeletal muscle couplon.

Curvature change as additional allosteric factor

Chen and Kudryashev (2020) demonstrated a measurably greater curvature in the open channel configuration (Fig. 6). The study also revealed transmembrane "extensions" or processes, presumably emanating from the RyR separate from the pore regions, the convergent movements of which could explain, to a degree, the changes in membrane curvature.

Under the simple assumption that this change extends to membrane regions under neighboring RyRs, the phenomenon may contribute to synchronization of channel opening, thus constituting an additional allosteric coupling mechanism. Indeed, that the opening of channel #1 causes the curvature of the underlying membrane to increase implies that the energy of an open channel #1 and its associated membrane is lower when said membrane is more curved. If this change in curvature extends to neighboring channel #2, it will favor the neighbor's opening. Deliberately simple calculations in Box 2 suggest that the change in curvature associated with RyR1 activation implements a significant allosteric coupling for both opening and closing.

Allostery in models of the cardiac couplon

As stated, the modeling of Ca^{2+} signaling in the heart has been more persistent, complex, and ambitious than for skeletal muscle; indeed, it starts from molecular gating, then takes on subcellular junctions, myocytes, syncytia of atria and ventricles, the conduction system, and the whole organ, in assumed "health" and various "disease" conditions. Qu et al. (2022) published an extensive review of this large modeling field. Here, I will just examine models that invoke allosteric interactions in addition to the ubiquitous effects of Ca^{2+}.

To my knowledge, the first of such models was proposed by Stern et al. (1999). Curiously, the allosteric effect there was included as a way to achieve timely termination of Ca^{2+} sparks, without concerns for their activation. Even though this contribution crystallized a collective effort, with ideas from earlier work on skeletal (Stern et al., 1997; Ríos et al., 1993; Shirokov et al., 1993) and cardiac muscle (Jafri et al., 1998; Imredy and Yue, 1994; Keizer and Levine, 1996), the one to formalize the scheme was bound to be Mike Stern, as he had warned the field about the difficulties of CICR termination even before Ca^{2+} sparks were known (Stern, 1992).

While the addition of allostery to the cluster model allowed a better fit to spark termination, a greater consequence was the adoption and generalization of the formalism in subsequent work. A characteristic of Stern's 1999 approach is that it is molecularly detailed, suitable to analyze groups as small as pairs (hence adequate to interpret the pauci-channel phenomena in bilayers), but also scalable to larger sets. Other models renounce the detailed approach in favor of features designed for clusters. A good example is the approach by Sobie et al. (2002), which accomplished impressive simulation of sparks but included allostery via terms that depended on collective rather than detailed properties of the cluster (i.e., fraction of channels open or closed).

Stern et al. (1999) incorporated allostery by introducing a free energy of interaction between neighboring tetramers that alters their gating transition rates. The magnitude of the term depended exclusively on the states of the RyRs in contact. To maintain microscopic reversibility in an energetically closed system, this term must be symmetrical, i.e., if the energy of *open* "tetramer 1" included a term ε contributed by *closed* "tetramer 2," the same ε had to be added to the energy balance of tetramer 2 when states of the pair were reversed. While microscopic reversibility is desirable for a purely allosteric transition when no external sources of energy are present, it is by no means required if Ca^{2+} gradients (Rengifo et al., 2002; G. Conradi Smith, personal communication) or electrical sensor movements are added to the mix.

The 26 years passed since the introduction of quantitative allostery as a hypothesis, specifically for cardiac muscle, has not seen much progress in answering whether it has any physiological or pathophysiological relevance. The problem is difficult for cardiac RyRs for multiple reasons: the prominent role of activation by Ca^{2+}, in tandem with marked Ca^{2+} depletion during Ca^{2+} release (e.g., Sobie et al., 2002; Sobie and Lederer, 2012), which makes formal accounting for CICR more difficult, the practical barriers to gathering currents in the ion's absence, and the lack of evidence of biochemically well-defined, stoichiometric inter-RyR2 links (as reviewed in the previous section). The extant research also failed to reveal a definite pharmacologic intervention that could prevent allostery or promote it. In spite of these difficulties, here I will recall in some detail contributions by Groff and Smith (2008) because they offer predictions that can be compared with experimental observations and because their clear formalization provides tools that should help in future modeling work.

As argued, skeletal muscle provides the more favorable scenario, both for having relevant allostery and for its demonstration. For these reasons, as I describe the existing modeling formalism for cardiac RyRs, I will note their suitability to skeletal muscle couplons and stress the simplifications that result from dropping the Ca^{2+}-dependent components, which is appropriate for skeletal muscle.

The simulation of coupled channel currents

The approach starts from a state diagram of the channel, which in this case will simply be

$$C \underset{k^-}{\overset{k^+}{\rightleftarrows}} O \qquad (4)$$

with unidirectional transition rates reflecting the intrinsic tendencies to open or close the isolated channel. When two channels are considered, they could evolve independently as shown in Scheme 1 at left, or gate in coupled fashion, which first implies a shift in the equilibrium of the transition, favoring for instance the opening of one when the other is open (i.e., the state *OO* of the pair favored over *OC* and *CO*). The assumption is made consistent with physics by assigning it to a change in free energies—an ε_{OO} of the pair of open channels more negative than the ε_{OC} applicable when one channel is open. More on the theory is presented in Box 3.

In sum, the model assumes changes in free energy that enter as exponential factors modifying the intrinsic transition rates, as

Box 3. **Energetics and kinetics of allostery**

The closed ⟷ open equilibrium of "channel 1" is altered in favor of the open state when free energy ε_{OO} (in units of kT), applicable when the allosterically coupled neighbor is open, is less than ε_{OO}, applicable when the neighbor is closed. The change in equilibrium constant is represented as a factor $e^{-(\varepsilon_{OO}-\varepsilon_{OC})}$, >1 to favor the *OO* state. Similarly, if "closed" were promoted by a closed partner, the term (ε_{CC}-ε_{OC}) would be negative. Assumptions that favor *CC* or *OO* are not mutually exclusive.

To introduce kinetics, an adjustable factor ν (the "splitting coefficient," Stern et al., 1999) is added to one of the transition rates, and (1 − ν) to the opposite one so that the rate of the transition can be adjusted without changing the equilibrium. In Scheme 1, the allosteric energies are represented by the matrix ε. Microscopic reversibility requires that ε_{CO} and ε_{OC} be equal. Given the equality, and considering that ε_{CO} and ε_{OC} only appear in differences, they can be made equal to zero without any loss of generality.

in the transitions at right in Scheme 1. These rules can be generalized to channel arrays, where one tetramer may be linked to multiple others. As the simplest extension, Groff and Smith develop in detail the case of three channels. With Fig. 10, I share their example, together with two versions suitable for skeletal muscle couplons: a four-channel case (Fig. 10 B) in which every tetramer links to two others, and a generalized 2N-channel example (Fig. 10 C), in which every tetramer except the two pairs at both ends is conformationally linked to three others.

In both the three-channel example and the four-channel couplon, one channel is allosterically linked to two others; therefore, in both cases the allosteric energy in every channel consists of two additive terms. When the top channel in Fig. 10 A goes from closed to open, in a starting configuration with the other channels closed, it experiences a change of energy 2(ε_{CO} - ε_{CC}); the same difference would apply for the four-channel skeletal muscle couplon (Fig. 10 B) if channel #1 were to open from an all-channels closed configuration.

Adding Ca2+ to allostery. To include activation by Ca^{2+}, the two-state scheme (Eq. 4) channel is changed to

$$C \underset{k^-}{\overset{k^+ c^\eta}{\rightleftarrows}} O \qquad (5)$$

where c is the local [Ca^{2+}] at the cytosolic side, and η is the cooperativity of binding. At variance with the computation of allosteric effects, which emerge only from the set of mechanically linked channels, c must be computed collecting the contributions of every open channel. This calculation is fraught, mainly because all open channels in the cluster contribute to the local [Ca^{2+}], with contributions determined by diffusion over various distances, conditioned by the presence of buffers, mobile and fixed. The difficulties are usually negotiated by assumptions that simplify the buffer properties, ignore the transients (by assuming that they are fast relative to the gating times), linearize the equations for buffered diffusion (which allows for combining by the addition of the multiple sources), and flatten the couplon geometry.

With these simplifications, the evolution in time of any array of N channels with defined allosteric pairings and optional Ca^{2+} sensitivity can be described as an N-valued Markov chain $S(t)$, a succession of vectors or sets S of state values (one value, say *C* or *O*, per channel) determined by rules that depend only on the present set of states. (The case for assuming this memoryless feature of Markov chains is clearly stronger for the skeletal muscle system, where Ca^{2+} activation—a process with "memory"—is absent). Box 4 details the simulation technique, including matrix methods put together by Greg Smith that simplify the calculus and its scaling to large clusters.

Fig. 11 pairs currents from coupled cardiac channels (selected from Figs. 1 and 2) with three-channel simulations by Groff and Smith (2008). Even though the simulations were not intended to fit particular records, they match reasonably well the currents recorded by Gaburjaková and Gaburjaková (2010), except for dwell times that are much shorter in the simulation. Straightforward changes in parameter values, say, of the basic rate constants, would bring the times into better agreement. Of note: the agreement is better with the assumption that allosteric interactions stabilize both the *OO* and *CC* pairwise configurations (which requires that both ε_{OO} and ε_{CC} be <0).

Models like those of Stern et al. (1999) and Groff and Smith (2008) cannot reproduce *prima facie* the flicker-less currents reported by Marx et al. (2001), as shown in Fig. 1, or Marx et al.

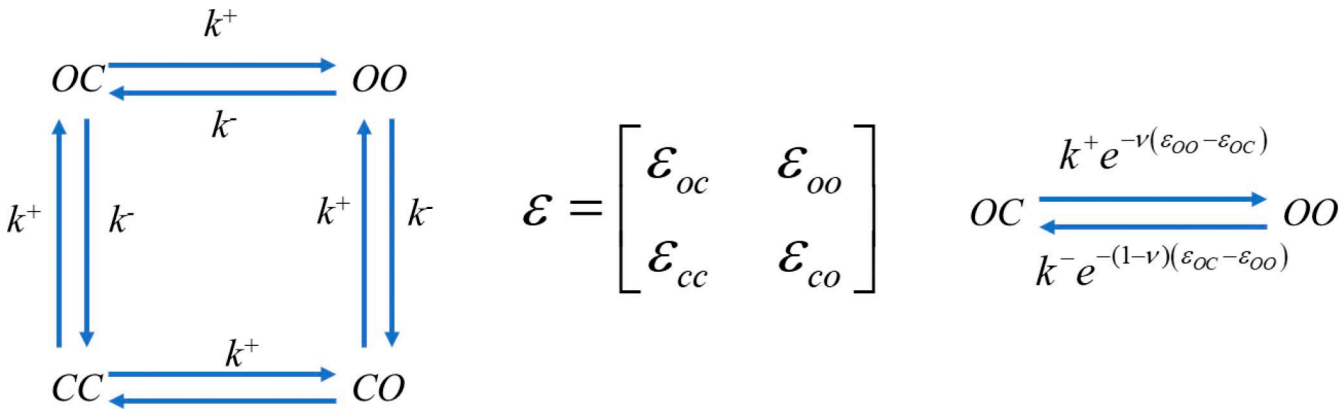

Scheme 1. Left: state diagram of a pair of 2-state channels gating independently. Center: the matrix of allosteric energies. Right: transitions linking two states of the pair, with allosteric factors (from Text Box 3) included in the transition rates.

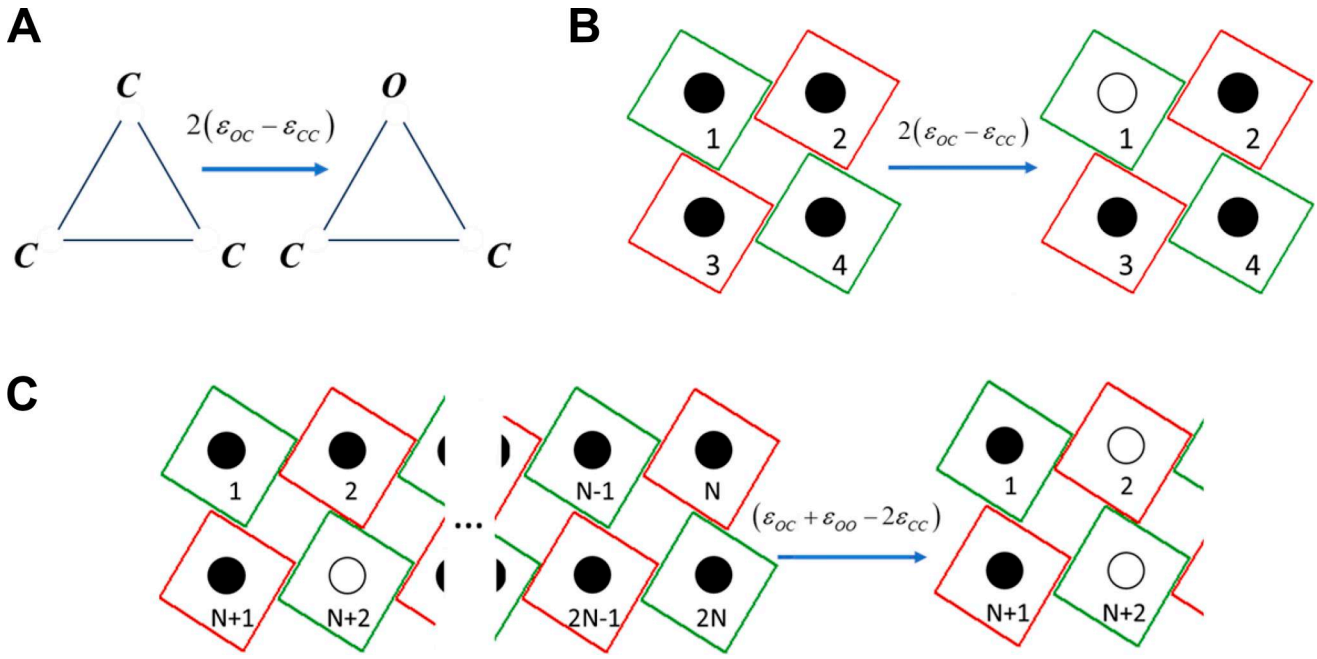

Figure 10. **Allosteric model rules in example couplons. (A)** Trio of RyRs, where each one interacts pairwise with the other two, transitions from configuration *CCC* to *OCC*. As indicated, the corresponding change in energy of the channel at top is $\Delta\varepsilon = 2(\varepsilon_{OO} - \varepsilon_{OC})$ in *kT* units. $e^{-v\Delta\varepsilon}$ enters as a factor the calculation of the rate of the forward transition. **(B)** Four-channel couplon, with the rules of interaction satisfied by RyR1s in skeletal muscle (RyRs of one color only interact with RyRs of the other color.). Under these rules, the opening of channel 1 has the same energy cost as the example in A. **(C)** Generic opening transition in a generic 2N-channel couplon with skeletal muscle array interaction rules. The energy cost of the transition represented, $\varepsilon_{OC} + \varepsilon_{OO} - 2\varepsilon_{CC}$, depends on both the initial and final array configurations. Panel A copies an example in Fig. 3 of Groff and Smith (2008).

(1998). The simple thermodynamic resource for suppressing the dwell times in *CO*/*OC*—the assumption of a high free energy in these states—would make the transitions unacceptably slow. The alternative is a direct $CC \longleftrightarrow OO$ conversion, contemplating a collective path to opening distinct from the individual molecular trajectories (a view, in passing, more consistent with the central idea in the MWC model of allostery, for which transitions are simultaneous). Again, the absence of flickering could be due instead to increased filtering imposed by a bilayer of larger surface area.

Higher level models of cardiac Ca^{2+} release. The modeling of currents through channels in small groups, comparable to bilayer-reconstituted currents, was taken one step further, to simulate Ca^{2+} sparks (Williams et al., 2011; Sobie et al., 2002; Sobie and Lederer, 2012; Stern et al., 1999; Groff and Smith, 2008).

Matching the many forms of Ca^{2+} release in heart muscle required complex assumptions that do not illuminate the relevance of allosteric coupling. Still, an overview of the work is useful, both to identify the difficulties and to preview experimental design that could finally probe inter-RyR2 allostery.

Box 4. **Monte Carlo simulation with kinetics**

The simulations are carried out as in Gillespie (1976), with operational details described in the Groff and Smith (2008) article. The evolution of the system is built via a series of successive stochastic decisions that require calculating transition rates for every channel in the set, to then decide what channel makes the transition. The decision is reached via lottery—a random variable uniformly distributed between 0 and 1 is applied to a segment of length 1 partitioned among the *N* channels according to their calculated rates.

To introduce kinetics consistent with the collection of calculated rates, the time of each transition is computed as the inverse of the *sum* of the individual rates.

Matrix algebra efficiently keeps track of the changes in interaction energies. The tools, for an *N* channel set, start from a state vector *S*, say [1,0,0,0] for $N = 4$, when only channel #1 is open. *S* and its complement, [0,1,1,1] in the example, put together as columns 2 and 1, respectively, constitute a 2 × N matrix Σ that changes to Σ_i as channel *i* makes the transition. An "adjacency" N × N matrix, A, represents the rules of contact; its element a_{mn} is 1 if channels *m* and *n* interact, 0 otherwise. Thus, for the trio in Fig. 10 A, the 3 × 3 matrix A has ones everywhere and zeros in the diagonal, whereas for the four-channel couplon in Fig. 10 B, it is

$$\mathbf{A} = \begin{bmatrix} 0 & 1 & 1 & 0 \\ 1 & 0 & 0 & 1 \\ 1 & 0 & 0 & 1 \\ 0 & 1 & 1 & 0 \end{bmatrix}$$

With these simple devices, plus the 2 × 2 matrix of energies ε defined in Scheme 1, the energy change when channel *i* makes its transition is just $\varepsilon \,.\, (\Sigma_i'\mathbf{A}\Sigma_i - \Sigma'\mathbf{A}\Sigma)$, where (′) indicates transposition and (.) an element-by-element multiplication followed by summation of all four elements in the 2 × 2 result matrix. The state-dependent rate of the transition in the channel of interest is calculated as the product of the intrinsic rate by the negative exponential of this value.

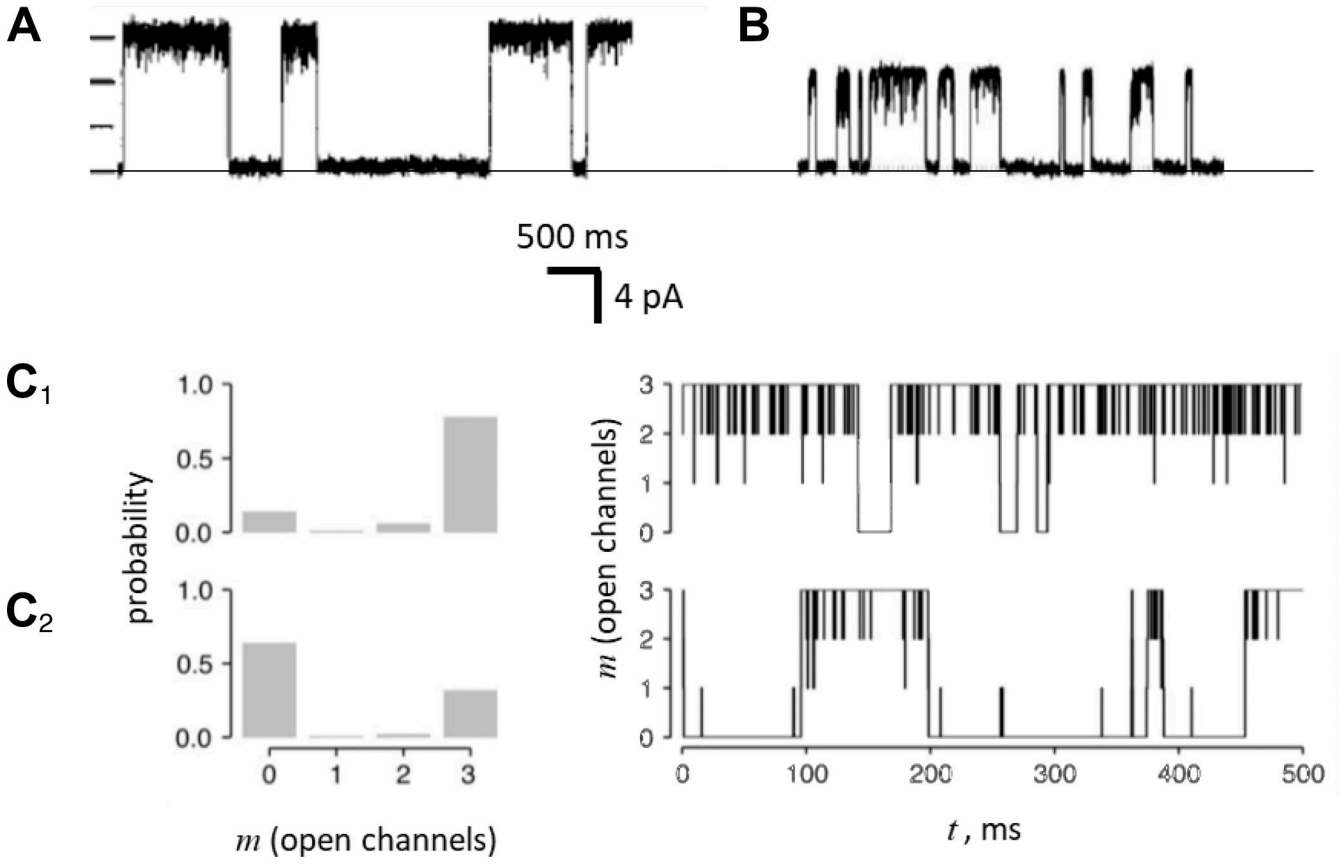

Figure 11. **Current records and simulations. (A)** Ca^{2+} current through a bilayer-reconstituted coupled RyR2 pair from dog heart in the presence of $[Ca^{2+}]_{cis}$ ~100 µM and $[Ca^{2+}]_{trans}$ ~50 mM. **(B)** Ca^{2+} current through a coupled RyR2 pair from rat heart, classified as "low activity," in the presence of $[Ca^{2+}]_{cis}$ = 170 µM and $[Ca^{2+}]_{trans}$ ~50 mM. C_1 and C_2, model currents, assuming the array of three channels represented in Fig. 10 A, with $\varepsilon_{OO} = -0.8$ and $\varepsilon_{CC} = \varepsilon_{OC} = \varepsilon_{CO} = 0$ (C_1) or $\varepsilon_{CC} = \varepsilon_{OO} = -0.8$ (C_2). The shaded bars represent the probability of configurations with *m* channels open. Panels A and B reproduce panels from Figs. 1 and 2. Panels C_1 and C_2 are reproduced from Fig. 3 in Groff and Smith (2008) by courtesy of Greg Conradi Smith. Fig. 11 is reprinted with permission from Elsevier.

Groff and Smith (2008) assume 25-channel "Cartesian" (i.e., square) arrays, with allostery between next neighbors as described above, and Ca^{2+} activation that specifies the increase in local $[Ca^{2+}]$ experienced by one channel when others are open, in any combination. The sum of these contributions, which like the set of allosteric energies must be recalculated at every step, constitutes a computational load that, as also shown in the studies of Sobie et al. (2002), can be replaced by a simpler "mean-field" calculation. In it, the channel-by-channel calculation is eschewed in favor of a simpler accounting of averaged local $[Ca^{2+}]$ and allosteric energies that depend only on the number of open (and closed) channels. Mean-field simplifications proved crucial for simulating arrays with large numbers of channels.

Either detailed or mean-field, these simulations produce release events consistent with the basic properties of Ca^{2+} sparks and show how allostery can modify them. The clearest emergent is the effect of interactions that stabilize closed pairs (i.e., large negative ε_{CC}) as insurers of robust spark termination. Of course, coupled opening (large negative ε_{OO}) favors spark formation. Also, stabilization (of open or closed pairs) always promotes the generation of spark-type events, as opposed to spread-out, uncoordinated openings.

Most encouraging for defining the role and relevance of allostery is the exercise that Groff and Smith called "washout of allosteric interactions," whereby they plotted spark parameters (duration, interspark interval, and frequency) as they progressively weakened the interaction. The washout effects compare favorably with observations, by J. Lederer and others, of the effects of the immunophilins and their ligands on spark parameters and general stability of Ca^{2+} release (e.g., Wehrens et al., 2003; Brillantes et al., 1994; Lehnart et al., 2008). My enthusiasm for this systematic approach is tempered by the observation, repeated in different scenarios, that most changes in parameters resulting from allostery can be offset, copied, enhanced, or reversed by adequate changes in the strength of coupling by Ca^{2+}, even without any resort to inactivation or more exotic assumptions.

Conclusions

(1) There is no robust evidence of a substantial role of inter-RyR allostery in skeletal or cardiac muscle physiology. There is, instead, good evidence that RyR channels can and do interact allosterically.

(2) The channels interact when reconstituted in bilayers; the interactions are difficult to observe and even more difficult to identify as truly allosteric—occurring without mediation by Ca^{2+}. In a few laboratories, the interaction has been observed with Ba^{2+} currents, which excludes CICR effects. They have also been observed at close to physiological [Ca^{2+}], with properties similar to those of independently gated currents. These observations leave open the possibility of a physiological role.
(3) The profiles of coupled currents vary with the observing laboratory and RyR isoform. Specifically, the number of coupled channels varies and the degree of interaction ranges from full coupling (seen with RyR2) to partial interactions (RyR1). This difference detracts from the possible relevance of these phenomena as it is opposite to the structural evidence of more regular and tighter pairings in native channel clusters of skeletal muscle.
(4) The inter-RyR interactions stand on a firm structural basis: the intrinsic ability of purified RyR tetramers to form ordered two-dimensional arrays, which, in the RyR1 case, mimic those found in native muscle.
(5) RyR1 and RyR2 tetramers show different dimerization rules: multiple interaction geometries are found for the cardiac isoform, but only the checkerboard interaction is found in native skeletal muscle junctions. The divergence extends to the RyR domains involved in the interactions, which notably include FKBP12.6 (or presumably FKBP12 when present) in RyR2–RyR2 contacts, but not in the inter-RyR1 contacts.
(6) Clusters of RyR2 in native membranes show different contact patterns, the prevalence of which varies with phosphorylation and the presence of FKBP12, correlated with changes in spark frequency and mass. These groupings are relatively loose, more suitable for activation by Ca^{2+} than allosteric interaction. So, again, there is interestingly modulated cooperativity, but no evidence of allostery.
(7) Molecular level modeling, developed for RyR2 groupings, has not contemplated inter-RyR allostery in isolation, but only as a complement to the established connections mediated by Ca^{2+}. Molecularly detailed models describe well the observations with few coupled channels in bilayers; when applied to larger clusters, they provide for reliable termination of Ca^{2+} sparks, and tailor their other features. I see this as proof of concept, but not of the actual operation of inter-RyR2 allostery in physiology.
(8) Recent studies confirm the decades-old picture of skeletal couplon structure, with its checkerboard array of RyRs and skipping overlap by DHPR voltage sensors, add evidence of an increased bending of the SR membrane, and, by MD simulations, show an increased "comfort" in the polymeric array upon channel opening. Both properties should be considered as mechanisms for pairwise coupled gating that favor the open state.

Perspectives

In sum, the promise of a significant role of inter-RyR allostery has been strengthened by the recent studies of structure, but there is still no robust evidence for it. What can be done? What sort of experiments or modeling can best probe the issue and fill this knowledge gap?

To probe inter-RyR2 allostery

So that I can end on a hopeful note, I will start from the cardiac field. There, I find the weakest evidence of allostery and the greatest difficulties to demonstrate or disprove its role. The main confounding factor is the pervasive control of gating by Ca^{2+}, made worse by the occurrence of Ca^{2+} depletion at the source, which makes the flux through open channels and the resultant feedbacks variable. The agonist cannot be removed, because without Ca^{2+} there is no cardiac EC coupling. Additionally, the loose and variable rules of clustering seem contrary to the tight contacts required for allostery. In particular, the most durable pairing does not satisfy the MWC allosteric protein criteria.

In spite of these challenging prospects, there is promise. Think of the continued improvement of optical approaches, which have now and for some time beat the "optical limit" of spatial resolution; or the possible development of molecular probes and mutational approaches at the increasingly precisely defined sites of interchannel contact. Interventions of this sort could be combined with the procedure delineated by Groff and Smith (2008) in their simulated washout of allosteric interactions, whereby they quantify the effects on spark statistics of progressively removing the interaction energy, as if the gradual removal of an agonist were abolishing allostery in a graded manner. If such an agonist existed, the richness and precision of the predictions would provide a robust test of validity of the assumptions. Groff and Smith put some faith on FKBP12.6 as agonist, and in the ability of RyR phosphorylation to gradually remove it. But much evidence runs against those views. Still, the "washout" predictions of Groff and Smith could be used to test whether mutational interventions or agonists are indeed altering an allosteric mechanism.

To probe inter-RyR1 allostery

The prospects are more hopeful for skeletal muscle, where the structural basis for contact and interaction is solid, and Ca^{2+} release can be used as readout without concern for interference by Ca^{2+}-dependent activation or local depletion (e.g., Zhou et al., 2005). What to ask for in a test? The simulated opening of channels in arrays of normal size (in the few-to-60-tetramer range) should match the detail of events at the couplon level; additionally, their simulated ensemble currents should be compared with the whole-cell Ca^{2+} release transient, a phenomenon that has been recorded and quantified by many labs in a variety of conditions, most precisely under voltage clamp.

In addition to matching the kinetics of Ca^{2+} release, which will require additional assumptions about inactivation, the simulations should recreate a defining property of skeletal EC coupling: Ca^{2+} release is graded with membrane voltage. The gradation should prevail at the nanodomain level; i.e., the individual couplons should respond incrementally to increasing depolarization, rather than by growing recruitment of fully

activated couplons, as in cardiac muscle. In plain terms, Ca^{2+} sparks, which occur when all channels in a couplon are activated, should not appear in the simulations. This condition seems difficult to satisfy, as a mechanism that couples channel openings is inherently explosive.

In other words, the successful model will have to realize the idea of a hierarchy of channels, first formulated cogently by Knox Chandler's group as follows: "*...a single voltage-gated SR channel, which is controlled by an apposing voltage sensor in the membrane of the transverse tubules, and adjacent SR channels that are not associated directly with voltage sensors but are slaved in an obligatory fashion to the voltage-gated SR channel. Coupling from the voltage-gated channel to its slaves could involve Ca, as suggested by* Rios and Pizarro (1988)*, or some other messenger*" (Pape et al., 1995). Because the hypothesis of mediation by Ca^{2+} has been proven wrong, we are left with allostery as the alternative "messenger" of choice.

Acknowledgments

Olaf S. Andersen served as editor.

As stated in Introduction, I had help from many colleagues: first, those who allowed republishing their figures and always enthusiastically clarified their techniques and concerns: the gating current pioneers, Andy Marks, Marta and Jana Gaburjaková, and Julio Copello; the structuralist pioneers Clara Franzini-Armstrong, Edwin Moore, and Montserrat Samsó, who made possible much of the work that came later; Filip Van Petegem, who in addition to illustrations shared many insights on structure–function; and Misha Kudryashev, Li Guohui, Zhu Yun, and Sun Fei, whose high-resolution studies contributed new evidence affirming the allostery between RyRs. This article owns much to Greg Conradi Smith, who beyond providing graphic material for two figures shared ideas on basic mechanism and helped me understand the ingenious formalism that allowed him to efficiently compute large models. Parisa Asghari clarified the process behind her lab's advanced descriptions of structure, and Chenyi Liao justified in detail the MD simulation that indicated allosteric favoring of open states. I also got help, ideas for more decisive research, and unguarded opinions, sometimes in the form of detailed documents worthy of publication (!!) from Mike Fill, Ana María Gómez, Jon Lederer, Saleet Jafri, Alexandra Zahradníková, Lothar Blatter, Susan Hamilton, Don Bers, Nagomi Kurebayashi, Héctor Valdivia, Takashi Murayama, Marta Gaburjaková, and Mike Stern. Thanks to Fred Cohen for help with the energetics of membrane bending, and to Bob Dirksen for his durable faith in the allosteric activation of orphan RyR1s. David Eisner, Carolina Figueroa, Christopher Lingle, Carlo Manno, and Eshwar Tammineni critiqued the manuscript and suggested many improvements.

Author contributions: Eduardo Rios: conceptualization, data curation, formal analysis, funding acquisition, investigation, methodology, project administration, resources, software, supervision, validation, visualization, and writing—original draft, review, and editing.

Disclosures: The author declares no competing interests exist.

Submitted: 22 August 2025
Revised: 3 November 2025
Accepted: 5 November 2025

References

Amador, F.J., S. Liu, N. Ishiyama, M.J. Plevin, A. Wilson, D.H. MacLennan, and M. Ikura. 2009. Crystal structure of type I ryanodine receptor amino-terminal beta-trefoil domain reveals a disease-associated mutation "hot spot" loop. *Proc. Natl. Acad. Sci. USA*. 106:11040–11044. https://doi.org/10.1073/pnas.0905186106

Asghari, P., D.R. Scriven, M. Ng, P. Panwar, K.C. Chou, F. van Petegem, and E.D. Moore. 2020. Cardiac ryanodine receptor distribution is dynamic and changed by auxiliary proteins and post-translational modification. *Elife*. 9:e51602. https://doi.org/10.7554/eLife.51602

Asghari, P., D.R.L. Scriven, S. Sanatani, S.K. Gandhi, A.I.M. Campbell, and E.D.W. Moore. 2014. Nonuniform and variable arrangements of ryanodine receptors within mammalian ventricular couplons. *Circ. Res.* 115:252–262. https://doi.org/10.1161/CIRCRESAHA.115.303897

Avila, G., E.H. Lee, C.F. Perez, P.D. Allen, and R.T. Dirksen. 2003. FKBP12 binding to RyR1 modulates excitation-contraction coupling in mouse skeletal myotubes. *J. Biol. Chem.* 278:22600–22608. https://doi.org/10.1074/jbc.M205866200

Baddeley, D., I. Jayasinghe, L. Lam, S. Rossberger, M.B. Cannell, and C. Soeller. 2009. Optical single-channel resolution imaging of the ryanodine receptor distribution in rat cardiac myocytes. *Proc. Natl. Acad. Sci. USA*. 106:22275–22280. https://doi.org/10.1073/pnas.0908971106

Baylor, S.M. 2005. Calcium sparks in skeletal muscle fibers. *Cell Calcium*. 37:513–530. https://doi.org/10.1016/j.ceca.2005.01.002

Bellinger, A.M., S. Reiken, C. Carlson, M. Mongillo, X. Liu, L. Rothman, S. Matecki, A. Lacampagne, and A.R. Marks. 2009. Hypernitrosylated ryanodine receptor calcium release channels are leaky in dystrophic muscle. *Nat. Med.* 15:325–330. https://doi.org/10.1038/nm.1916

Bers, D.M. 2012. Ryanodine receptor S2808 phosphorylation in heart failure: Smoking gun or red herring. *Circ. Res.* 110:796–799. https://doi.org/10.1161/CIRCRESAHA.112.265579

Blatter, L.A., J. Hüser, and E. Ríos. 1997. Sarcoplasmic reticulum Ca^{2+} release flux underlying Ca^{2+} sparks in cardiac muscle. *Proc. Natl. Acad. Sci. USA*. 94:4176–4181. https://doi.org/10.1073/pnas.94.8.4176

Block, B.A., T. Imagawa, K.P. Campbell, and C. Franzini-Armstrong. 1988. Structural evidence for direct interaction between the molecular components of the transverse tubule/sarcoplasmic reticulum junction in skeletal muscle. *J. Cell Biol.* 107:2587–2600. https://doi.org/10.1083/jcb.107.6.2587

Bray, D., and T. Duke. 2004. Conformational spread: The propagation of allosteric states in large multiprotein complexes. *Annu. Rev. Biophys. Biomol. Struct.* 33:53–73. https://doi.org/10.1146/annurev.biophys.33.110502.132703

Brillantes, A.B., K. Ondrias, A. Scott, E. Kobrinsky, E. Ondriasová, M.C. Moschella, T. Jayaraman, M. Landers, B.E. Ehrlich, and A.R. Marks. 1994. Stabilization of calcium release channel (ryanodine receptor) function by FK506-binding protein. *Cell*. 77:513–523. https://doi.org/10.1016/0092-8674(94)90214-3

Brown, E.J., M.W. Albers, T.B. Shin, K. Ichikawa, C.T. Keith, W.S. Lane, and S.L. Schreiber. 1994. A mammalian protein targeted by G1-arresting rapamycin-receptor complex. *Nature*. 369:756–758. https://doi.org/10.1038/369756a0

Cabra, V., T. Murayama, and M. Samsó. 2016. Ultrastructural analysis of self-associated RyR2s. *Biophys. J.* 110:2651–2662. https://doi.org/10.1016/j.bpj.2016.05.013

Canato, M., M. Scorzeto, M. Giacomello, F. Protasi, C. Reggiani, and G.J.M. Stienen. 2010. Massive alterations of sarcoplasmic reticulum free calcium in skeletal muscle fibers lacking calsequestrin revealed by a genetically encoded probe. *Proc. Natl. Acad. Sci. USA*. 107:22326–22331. https://doi.org/10.1073/pnas.1009168108

Cannell, M.B., H. Cheng, and W.J. Lederer. 1995. The control of calcium release in heart muscle. *Science*. 268:1045–1049. https://doi.org/10.1126/science.7754384

Chandler, W.K., R.F. Rakowski, and M.F. Schneider. 1976. Effects of glycerol treatment and maintained depolarization on charge movement in skeletal muscle. *J. Physiol.* 254:285–316. https://doi.org/10.1113/jphysiol.1976.sp011233

Changeux, J.P. 1961. The feedback control mechanisms of biosynthetic L-threonine deaminase by L-isoleucine. *Cold Spring Harb. Symp. Quant. Biol.* 26:313–318. https://doi.org/10.1101/sqb.1961.026.01.037

Changeux, J.-P. 2011. 50th anniversary of the word "Allosteric". *Protein Sci.* 20:1119–1124. https://doi.org/10.1002/pro.658
Changeux, J.-P. 2012. Allostery and the Monod-Wyman-Changeux model after 50 years. *Annu. Rev. Biophys.* 41:103–133. https://doi.org/10.1146/annurev-biophys-050511-102222
Chen, W., and M. Kudryashev. 2020. Structure of RyR1 in native membranes. *EMBO Rep.* 21:e49891. https://doi.org/10.15252/embr.201949891
Cheng, H., W.J. Lederer, and M.B. Cannell. 1993. Calcium sparks: Elementary events underlying excitation-contraction coupling in heart muscle. *Science*. 262:740–744. https://doi.org/10.1126/science.8235594
Dekker, J.P., and G. Yellen. 2006. Cooperative gating between single HCN pacemaker channels. *J. Gen. Physiol.* 128:561–567. https://doi.org/10.1085/jgp.200609599
Dixon, R.E., M.F. Navedo, M.D. Binder, and L.F. Santana. 2022. Mechanisms and physiological implications of cooperative gating of clustered ion channels. *Physiol. Rev.* 102:1159–1210. https://doi.org/10.1152/physrev.00022.2021
Duke, T.A., and D. Bray. 1999. Heightened sensitivity of a lattice of membrane receptors. *Proc. Natl. Acad. Sci. USA*. 96:10104–10108. https://doi.org/10.1073/pnas.96.18.10104
Duke, T.A., N. Le Novère, and D. Bray. 2001. Conformational spread in a ring of proteins: A stochastic approach to allostery. *J. Mol. Biol.* 308:541–553. https://doi.org/10.1006/jmbi.2001.4610
Efremov, R.G., A. Leitner, R. Aebersold, and S. Raunser. 2015. Architecture and conformational switch mechanism of the ryanodine receptor. *Nature*. 517:39–43. https://doi.org/10.1038/nature13916
Eisner, D., and E. Murphy. 2024. Honey, they shrunk the ATP. *Proc. Natl. Acad. Sci. USA*. 121:e2410446121. https://doi.org/10.1073/pnas.2410446121
Endo, M. 2009. Calcium-induced calcium release in skeletal muscle. *Physiol. Rev.* 89:1153–1176. https://doi.org/10.1152/physrev.00040.2008
Franzini-Armstrong, C., and G. Nunzi. 1983. Junctional feet and particles in the triads of a fast-twitch muscle fibre. *J. Muscle Res. Cell Motil.* 4:233–252. https://doi.org/10.1007/BF00712033
Franzini-Armstrong, C., F. Protasi, and V. Ramesh. 1999. Shape, size, and distribution of Ca(2+) release units and couplons in skeletal and cardiac muscles. *Biophys. J.* 77:1528–1539. https://doi.org/10.1016/S0006-3495(99)77000-1
Gaburjakova, J., and M. Gaburjakova. 2010. Identification of changes in the functional profile of the cardiac ryanodine receptor caused by the coupled gating phenomenon. *J. Membr. Biol.* 234:159–169. https://doi.org/10.1007/s00232-010-9243-8
Gaburjakova, M., J. Gaburjakova, S. Reiken, F. Huang, S.O. Marx, N. Rosemblit, and A.R. Marks. 2001. FKBP12 binding modulates ryanodine receptor channel gating. *J. Biol. Chem.* 276:16931–16935. https://doi.org/10.1074/jbc.M100856200
des Georges, A., O.B. Clarke, R. Zalk, Q. Yuan, K.J. Condon, R.A. Grassucci, W.A. Hendrickson, A.R. Marks, and J. Frank. 2016. Structural basis for gating and activation of RyR1. *Cell*. 167:145–157.e17. https://doi.org/10.1016/j.cell.2016.08.075
Gillespie, D.T. 1976. A general method for numerically simulating the stochastic time evolution of coupled chemical reactions. *J. Comput. Phys.* 22:403–439.
Goforth, R.L., A.K. Chi, D.V. Greathouse, L.L. Providence, R.E. Koeppe, and O.S. Andersen. 2003. Hydrophobic coupling of lipid bilayer energetics to channel function. *J. Gen. Physiol.* 121:477–493. https://doi.org/10.1085/jgp.200308797
Groff, J.R., and G.D. Smith. 2008. Ryanodine receptor allosteric coupling and the dynamics of calcium sparks. *Biophys. J.* 95:135–154. https://doi.org/10.1529/biophysj.107.119982
Guo, T., R.L. Cornea, S. Huke, E. Camors, Y. Yang, E. Picht, B.R. Fruen, and D.M. Bers. 2010. Kinetics of FKBP12.6 binding to ryanodine receptors in permeabilized cardiac myocytes and effects on Ca sparks. *Circ. Res.* 106:1743–1752. https://doi.org/10.1161/CIRCRESAHA.110.219816
Hayashi, T., M.E. Martone, Z. Yu, A. Thor, M. Doi, M.J. Holst, M.H. Ellisman, and M. Hoshijima. 2009. Three-dimensional electron microscopy reveals new details of membrane systems for Ca^{2+} signaling in the heart. *J. Cell Sci.* 122:1005–1013. https://doi.org/10.1242/jcs.028175
Heiss, M.C., M.L. Fernandeź-Quintero, M. Campiglio, Y. El Ghaleb, S. Pelizzari, J.R. Loeffler, K.R. Liedl, P. Tuluc, and B.E. Flucher. 2025. Voltage sensor gating charge interactions bimodally regulate voltage-dependence and kinetics of calcium channel activation. *J. Gen. Physiol.* 157:e202513769. https://doi.org/10.1085/jgp.202513769
Helfrich, W. 1973. Elastic properties of lipid bilayers: theory and possible experiments. *Z. Naturforsch. C*. 28:693–703. https://doi.org/10.1515/znc-1973-11-1209
Hernández-Ochoa, E.O., and M.F. Schneider. 2012. Voltage clamp methods for the study of membrane currents and SR Ca(2+) release in adult skeletal muscle fibres. *Prog. Biophys. Mol. Biol.* 108:98–118. https://doi.org/10.1016/j.pbiomolbio.2012.01.001
Imredy, J.P., and D.T. Yue. 1994. Mechanism of Ca^{2+}-sensitive inactivation of L-type Ca^{2+} channels. *Neuron*. 12:1301–1318. https://doi.org/10.1016/0896-6273(94)90446-4
Jafri, M.S., J.J. Rice, and R.L. Winslow. 1998. Cardiac Ca^{2+} dynamics: The roles of ryanodine receptor adaptation and sarcoplasmic reticulum load. *Biophys. J.* 74:1149–1168. https://doi.org/10.1016/S0006-3495(98)77832-4
Jayaraman, T., A.M. Brillantes, A.P. Timerman, S. Fleischer, H. Erdjument-Bromage, P. Tempst, and A.R. Marks. 1992. FK506 binding protein associated with the calcium release channel (ryanodine receptor). *J. Biol. Chem.* 267:9474–9477.
Jiang, Y.H., M.G. Klein, and M.F. Schneider. 1999. Numerical simulation of Ca^{2+} "sparks" in skeletal muscle. *Biophys. J.* 77:2333–2357. https://doi.org/10.1016/s0006-3495(99)77072-4
Keizer, J., and L. Levine. 1996. Ryanodine receptor adaptation and Ca^{2+}(-)induced Ca^{2+} release-dependent Ca^{2+} oscillations. *Biophys. J.* 71:3477–3487. https://doi.org/10.1016/S0006-3495(96)79543-7
Kettlun, C., A. González, E. Ríos, and M. Fill. 2003. Unitary Ca^{2+} current through mammalian cardiac and amphibian skeletal muscle ryanodine receptor Channels under near-physiological ionic conditions. *J. Gen. Physiol.* 122:407–417. https://doi.org/10.1085/jgp.200308843
Klein, M.G., H. Cheng, L.F. Santana, Y.H. Jiang, W.J. Lederer, and M.F. Schneider. 1996. Two mechanisms of quantized calcium release in skeletal muscle. *Nature*. 379:455–458. https://doi.org/10.1038/379455a0
Krouse, M.E., and J.J. Wine. 2001. Evidence that CFTR channels can regulate the open duration of other CFTR channels: cooperativity. *J. Membr. Biol.* 182:223–232. https://doi.org/10.1007/s00232-001-0046-9
Lam, E., M.M. Martin, A.P. Timerman, C. Sabers, S. Fleischer, T. Lukas, R.T. Abraham, S.J. O'Keefe, E.A. O'Neill, and G.J. Wiederrecht. 1995. A novel FK506 binding protein can mediate the immunosuppressive effects of FK506 and is associated with the cardiac ryanodine receptor. *J. Biol. Chem.* 270:26511–26522. https://doi.org/10.1074/jbc.270.44.26511
Laver, D.R., E.R. O'Neill, and G.D. Lamb. 2004. Luminal Ca^{2+}-regulated Mg^{2+} inhibition of skeletal RyRs reconstituted as isolated channels or coupled clusters. *J. Gen. Physiol.* 124:741–758. https://doi.org/10.1085/jgp.200409092
Lehnart, S.E., M. Mongillo, A. Bellinger, N. Lindegger, B.-X. Chen, W. Hsueh, S. Reiken, A. Wronska, L.J. Drew, C.W. Ward, et al. 2008. Leaky Ca^{2+} release channel/ryanodine receptor 2 causes seizures and sudden cardiac death in mice. *J. Clin. Invest.* 118:2230–2245. https://doi.org/10.1172/JCI35346
Liu, J., J.D. Farmer, W.S. Lane, J. Friedman, I. Weissman, and S.L. Schreiber. 1991. Calcineurin is a common target of cyclophilin-cyclosporin A and FKBP-FK506 complexes. *Cell*. 66:807–815. https://doi.org/10.1016/0092-8674(91)90124-h
Loesser, K.E., L. Castellani, and C. Franzini-Armstrong. 1992. Dispositions of junctional feet in muscles of invertebrates. *J. Muscle Res. Cell Motil.* 13:161–173. https://doi.org/10.1007/BF01874153
Marko, M., C. Hsieh, R. Schalek, J. Frank, and C. Mannella. 2007. Focused-ion-beam thinning of frozen-hydrated biological specimens for cryo-electron microscopy. *Nat. Methods*. 4:215–217. https://doi.org/10.1038/nmeth1014
Marx, S.O., J. Gaburjakova, M. Gaburjakova, C. Henrikson, K. Ondrias, and A.R. Marks. 2001. Coupled gating between cardiac calcium release channels (ryanodine receptors). *Circ. Res.* 88:1151–1158. https://doi.org/10.1161/hh1101.091268
Marx, S.O., K. Ondrias, and A.R. Marks. 1998. Coupled gating between individual skeletal muscle Ca^{2+} release channels (Ryanodine receptors). *Science*. 281:818–821. https://doi.org/10.1126/science.281.5378.818
Marx, S.O., S. Reiken, Y. Hisamatsu, T. Jayaraman, D. Burkhoff, N. Rosemblit, and A.R. Marks. 2000. PKA phosphorylation dissociates FKBP12.6 from the calcium release channel (ryanodine receptor): Defective regulation in failing hearts. *Cell*. 101:365–376. https://doi.org/10.1016/s0092-8674(00)80847-8
Mejía-Alvarez, R., C. Kettlun, E. Ríos, M. Stern, and M. Fill. 1999. Unitary Ca^{2+} current through cardiac ryanodine receptor channels under quasi-physiological ionic conditions. *J. Gen. Physiol.* 113:177–186. https://doi.org/10.1085/jgp.113.2.177
Molina, M.L., F.N. Barrera, A.M. Fernández, J.A. Poveda, M.L. Renart, J.A. Encinar, G. Riquelme, and J.M. González-Ros. 2006. Clustering and coupled gating modulate the activity in KcsA, a potassium channel model. *J. Biol. Chem.* 281:18837–18848. https://doi.org/10.1074/jbc.M600342200

Monod, J., J. Wyman, and J.P. Changeux. 1965. ON the nature of allosteric transitions: A plausible model. *J. Mol. Biol.* 12:88–118. https://doi.org/10.1016/s0022-2836(65)80285-6

Murayama, T., and N. Kurebayashi. 2011. Two ryanodine receptor isoforms in nonmammalian vertebrate skeletal muscle: Possible roles in excitation-contraction coupling and other processes. *Prog. Biophys. Mol. Biol.* 105: 134–144. https://doi.org/10.1016/j.pbiomolbio.2010.10.003

Nakai, J., R.T. Dirksen, H.T. Nguyen, I.N. Pessah, K.G. Beam, and P.D. Allen. 1996. Enhanced dihydropyridine receptor channel activity in the presence of ryanodine receptor. *Nature*. 380:72–75. https://doi.org/10.1038/380072a0

Naundorf, B., F. Wolf, and M. Volgushev. 2006. Unique features of action potential initiation in cortical neurons. *Nature*. 440:1060–1063. https://doi.org/10.1038/nature04610

Navedo, M.F., E.P. Cheng, C. Yuan, S. Votaw, J.D. Molkentin, J.D. Scott, and L.F. Santana. 2010. Increased coupled gating of L-type Ca^{2+} channels during hypertension and Timothy syndrome. *Circ. Res.* 106:748–756. https://doi.org/10.1161/CIRCRESAHA.109.213363

Nelson, M.T., H. Cheng, M. Rubart, L.F. Santana, A.D. Bonev, H.J. Knot, and W.J. Lederer. 1995. Relaxation of arterial smooth muscle by calcium sparks. *Science*. 270:633–637. https://doi.org/10.1126/science.270.5236.633

Ondrias, K., and A. Mojzisová. 2002. Coupled gating between individual cardiac ryanodine calcium release channels. *Gen. Physiol. Biophys.* 21: 73–84.

Pape, P.C., D.S. Jong, and W.K. Chandler. 1995. Calcium release and its voltage dependence in frog cut muscle fibers equilibrated with 20 mM EGTA. *J. Gen. Physiol.* 106:259–336. https://doi.org/10.1085/jgp.106.2.259

Pelizzari, S., M.C. Heiss, M.L. Fernández-Quintero, Y. El Ghaleb, K.R. Liedl, P. Tuluc, M. Campiglio, and B.E. Flucher. 2024. CaV1.1 voltage-sensing domain III exclusively controls skeletal muscle excitation-contraction coupling. *Nat. Commun.* 15:7440. https://doi.org/10.1038/s41467-024-51809-5

Peng, W., H. Shen, J. Wu, W. Guo, X. Pan, R. Wang, S.R.W. Chen, and N. Yan. 2016. Structural basis for the gating mechanism of the type 2 ryanodine receptor RyR2. *Science*. 354:aah5324. https://doi.org/10.1126/science.aah5324

Porta, M., P.L. Diaz-Sylvester, J.T. Neumann, A.L. Escobar, S. Fleischer, and J.A. Copello. 2012. Coupled gating of skeletal muscle ryanodine receptors is modulated by Ca^{2+}, Mg^{2+}, and ATP. *Am. J. Physiol. Cell Physiol.* 303:C682–C697. https://doi.org/10.1152/ajpcell.00150.2012

Qu, Z., D. Yan, and Z. Song. 2022. Modeling calcium cycling in the heart: Progress, pitfalls, and challenges. *Biomolecules*. 12:1686. https://doi.org/10.3390/biom12111686

Rengifo, J., R. Rosales, A. González, H. Cheng, M.D. Stern, and E. Ríos. 2002. Intracellular Ca(2+) release as irreversible Markov process. *Biophys. J.* 83:2511–2521. https://doi.org/10.1016/S0006-3495(02)75262-4

Renken, C., C.-E. Hsieh, M. Marko, B. Rath, A. Leith, T. Wagenknecht, J. Frank, and C.A. Mannella. 2009. Structure of frozen-hydrated triad junctions: A case study in motif searching inside tomograms. *J. Struct. Biol.* 165:53–63. https://doi.org/10.1016/j.jsb.2008.09.011

Rhana, P., C. Matsumoto, Z. Fong, A.D. Costa, S.G. Del Villar, R.E. Dixon, and L.F. Santana. 2024. Fueling the heartbeat: Dynamic regulation of intracellular ATP during excitation-contraction coupling in ventricular myocytes. *Proc. Natl. Acad. Sci. USA*. 121:e2318535121. https://doi.org/10.1073/pnas.2318535121

Ríos, E. 2018. Calcium-induced release of calcium in muscle: 50 years of work and the emerging consensus. *J. Gen. Physiol.* 150:521–537. https://doi.org/10.1085/jgp.201711959

Rios, E., and G. Brum. 1987. Involvement of dihydropyridine receptors in excitation-contraction coupling in skeletal muscle. *Nature*. 325:717–720. https://doi.org/10.1038/325717a0

Ríos, E., D. Gillespie, and C. Franzini-Armstrong. 2019. The binding interactions that maintain excitation-contraction coupling junctions in skeletal muscle. *J. Gen. Physiol.* 151:593–605. https://doi.org/10.1085/jgp.201812268

Ríos, E., M. Karhanek, J. Ma, and A. González. 1993. An allosteric model of the molecular interactions of excitation-contraction coupling in skeletal muscle. *J. Gen. Physiol.* 102:449–481. https://doi.org/10.1085/jgp.102.3.449

Rios, E., and G. Pizarro. 1988. Voltage sensors and calcium channels of excitation-contraction coupling. *Physiology*. 3:223–227. https://doi.org/10.1152/physiologyonline.1988.3.6.223

Ríos, E., M.D. Stern, A. González, G. Pizarro, and N. Shirokova. 1999. Calcium release flux underlying Ca^{2+} sparks of frog skeletal muscle. *J. Gen. Physiol.* 114:31–48. https://doi.org/10.1085/jgp.114.1.31

Samsó, M., W. Feng, I.N. Pessah, and P.D. Allen. 2009. Coordinated movement of cytoplasmic and transmembrane domains of RyR1 upon gating. *PLoS Biol.* 7:e85. https://doi.org/10.1371/journal.pbio.1000085

Shirokov, R., R. Levis, N. Shirokova, and E. Ríos. 1993. Ca(2+)-dependent inactivation of cardiac L-type Ca^{2+} channels does not affect their voltage sensor. *J. Gen. Physiol.* 102:1005–1030. https://doi.org/10.1085/jgp.102.6.1005

Shirokova, N., J. García, G. Pizarro, and E. Ríos. 1996. Ca^{2+} release from the sarcoplasmic reticulum compared in amphibian and mammalian skeletal muscle. *J. Gen. Physiol.* 107:1–18. https://doi.org/10.1085/jgp.107.1.1

Sobie, E.A., K.W. Dilly, J. dos Santos Cruz, W.J. Lederer, and M.S. Jafri. 2002. Termination of cardiac Ca(2+) sparks: An investigative mathematical model of calcium-induced calcium release. *Biophys. J.* 83:59–78. https://doi.org/10.1016/s0006-3495(02)75149-7

Sobie, E.A., and W.J. Lederer. 2012. Dynamic local changes in sarcoplasmic reticulum calcium: Physiological and pathophysiological roles. *J. Mol. Cell. Cardiol.* 52:304–311. https://doi.org/10.1016/j.yjmcc.2011.06.024

Soeller, C., and M.B. Cannell. 2002. Estimation of the sarcoplasmic reticulum Ca^{2+} release flux underlying Ca^{2+} sparks. *Biophys. J.* 82:2396–2414. https://doi.org/10.1016/S0006-3495(02)75584-7

Steele, T.W.E., and M. Samsó. 2019. The FKBP12 subunit modifies the long-range allosterism of the ryanodine receptor. *J. Struct. Biol.* 205:180–188. https://doi.org/10.1016/j.jsb.2018.12.007

Stephenson, D.G. 2024. Modeling the mechanism of Ca^{2+} release in skeletal muscle by DHPRs easing inhibition at RyR I1-sites. *J. Gen. Physiol.* 156: e202213113. https://doi.org/10.1085/jgp.202213113

Stern, M.D. 1992. Theory of excitation-contraction coupling in cardiac muscle. *Biophys. J.* 63:497–517. https://doi.org/10.1016/S0006-3495(92)81615-6

Stern, M.D., G. Pizarro, and E. Ríos. 1997. Local control model of excitation-contraction coupling in skeletal muscle. *J. Gen. Physiol.* 110:415–440. https://doi.org/10.1085/jgp.110.4.415

Stern, M.D., L.S. Song, H. Cheng, J.S. Sham, H.T. Yang, K.R. Boheler, and E. Ríos. 1999. Local control models of cardiac excitation-contraction coupling. A possible role for allosteric interactions between ryanodine receptors. *J. Gen. Physiol.* 113:469–489. https://doi.org/10.1085/jgp.113.3.469

Sztretye, M., J. Yi, L. Figueroa, J. Zhou, L. Royer, P. Allen, G. Brum, and E. Ríos. 2011. Measurement of RyR permeability reveals a role of calsequestrin in termination of SR Ca(2+) release in skeletal muscle. *J. Gen. Physiol.* 138:231–247. https://doi.org/10.1085/jgp.201010592

Tanabe, T., K.G. Beam, J.A. Powell, and S. Numa. 1988. Restoration of excitation-contraction coupling and slow calcium current in dysgenic muscle by dihydropyridine receptor complementary DNA. *Nature*. 336: 134–139. https://doi.org/10.1038/336134a0

Tang, W., C.P. Ingalls, W.J. Durham, J. Snider, M.B. Reid, G. Wu, M.M. Matzuk, and S.L. Hamilton. 2004. Altered excitation-contraction coupling with skeletal muscle specific FKBP12 deficiency. *FASEB J.* 18:1597–1599. https://doi.org/10.1096/fj.04-1587fje

Timerman, A.P., H. Onoue, H.B. Xin, S. Barg, J. Copello, G. Wiederrecht, and S. Fleischer. 1996. Selective binding of FKBP12.6 by the cardiac ryanodine receptor. *J. Biol. Chem.* 271:20385–20391. https://doi.org/10.1074/jbc.271.34.20385

Tsugorka, A., E. Ríos, and L.A. Blatter. 1995. Imaging elementary events of calcium release in skeletal muscle cells. *Science*. 269:1723–1726. https://doi.org/10.1126/science.7569901

Tung, C.-C., P.A. Lobo, L. Kimlicka, and F. Van Petegem. 2010. The amino-terminal disease hotspot of ryanodine receptors forms a cytoplasmic vestibule. *Nature*. 468:585–588. https://doi.org/10.1038/nature09471

Vierra, N.C., S.C. O'Dwyer, C. Matsumoto, L.F. Santana, and J.S. Trimmer. 2021. Regulation of neuronal excitation–transcription coupling by Kv2.1-induced clustering of somatic L-type Ca^{2+} channels at ER-PM junctions. *Proc. Natl. Acad. Sci. USA*. 118:e2110094118. https://doi.org/10.1073/pnas.2110094118

Wagenknecht, T., R. Grassucci, J. Berkowitz, G.J. Wiederrecht, H.B. Xin, and S. Fleischer. 1996. Cryoelectron microscopy resolves FK506-binding protein sites on the skeletal muscle ryanodine receptor. *Biophys. J.* 70: 1709–1715. https://doi.org/10.1016/S0006-3495(96)79733-3

Wagenknecht, T., C. Hsieh, and M. Marko. 2015. Skeletal muscle triad junction ultrastructure by Focused-Ion-Beam milling of muscle and Cryo-Electron Tomography. *Eur. J. Transl. Myol.* 25:4823. https://doi.org/10.4081/ejtm.2015.4823

Wagenknecht, T., C.-E. Hsieh, B.K. Rath, S. Fleischer, and M. Marko. 2002. Electron tomography of frozen-hydrated isolated triad junctions. *Biophys. J.* 83:2491–2501. https://doi.org/10.1016/S0006-3495(02)75260-0

Wehrens, X.H.T., S.E. Lehnart, F. Huang, J.A. Vest, S.R. Reiken, P.J. Mohler, J. Sun, S. Guatimosim, L.S. Song, N. Rosemblit, et al. 2003. FKBP12.6 deficiency and defective calcium release channel (ryanodine receptor) function linked to exercise-induced sudden cardiac death. *Cell*. 113: 829–840. https://doi.org/10.1016/s0092-8674(03)00434-3

Wehrens, X.H.T., S.E. Lehnart, S. Reiken, R. van der Nagel, R. Morales, J. Sun, Z. Cheng, S.-X. Deng, L.J. de Windt, D.W. Landry, and A.R. Marks. 2005. Enhancing calstabin binding to ryanodine receptors improves cardiac and skeletal muscle function in heart failure. *Proc. Natl. Acad. Sci. USA*. 102:9607–9612. https://doi.org/10.1073/pnas.0500353102

Wehrens, X.H.T., S.E. Lehnart, S.R. Reiken, S.-X. Deng, J.A. Vest, D. Cervantes, J. Coromilas, D.W. Landry, and A.R. Marks. 2004. Protection from cardiac Arrhythmia through ryanodine receptor-stabilizing protein Calstabin2. *Science*. 304:292–296. https://doi.org/10.1126/science.1094301

Williams, G.S.B., A.C. Chikando, H.-T.M. Tuan, E.A. Sobie, W.J. Lederer, and M.S. Jafri. 2011. Dynamics of calcium sparks and calcium leak in the heart. *Biophys. J.* 101:1287–1296. https://doi.org/10.1016/j.bpj.2011.07.021

Woll, K.A., and F. Van Petegem. 2022. Calcium-release channels: Structure and function of IP3 receptors and ryanodine receptors. *Physiol. Rev.* 102: 209–268. https://doi.org/10.1152/physrev.00033.2020

Xiao, J., X. Tian, P.P. Jones, J. Bolstad, H. Kong, R. Wang, L. Zhang, H.J. Duff, A.M. Gillis, S. Fleischer, et al. 2007. Removal of FKBP12.6 does not alter the conductance and activation of the cardiac ryanodine receptor or the susceptibility to stress-induced ventricular arrhythmias. *J. Biol. Chem.* 282:34828–34838. https://doi.org/10.1074/jbc.M707423200

Xu, J., C. Liao, C.-C. Yin, G. Li, Y. Zhu, and F. Sun. 2024. In situ structural insights into the excitation-contraction coupling mechanism of skeletal muscle. *Sci. Adv.* 10:eadl1126. https://doi.org/10.1126/sciadv.adl1126

Yan, Z., X. Bai, C. Yan, J. Wu, Z. Li, T. Xie, W. Peng, C. Yin, X. Li, S.H.W. Scheres, et al. 2015. Structure of the rabbit ryanodine receptor RyR1 at near-atomic resolution. *Nature*. 517:50–55. https://doi.org/10.1038/nature14063

Yin, C.-C., L.G. D'Cruz, and F.A. Lai. 2008. Ryanodine receptor arrays: Not just a pretty pattern? *Trends Cell Biol.* 18:149–156. https://doi.org/10.1016/j.tcb.2008.02.003

Yuchi, Z., S.M.W.K. Yuen, K. Lau, A.Q. Underhill, R.L. Cornea, J.D. Fessenden, and F. Van Petegem. 2015. Crystal structures of ryanodine receptor SPRY1 and tandem-repeat domains reveal a critical FKBP12 binding determinant. *Nat. Commun.* 6:7947. https://doi.org/10.1038/ncomms8947

Zahradníková, A., M. Gaburjáková, J.H.B. Bridge, and I. Zahradník. 2010. Challenging quantal calcium signaling in cardiac myocytes. *J. Gen. Physiol.* 136:581–583. https://doi.org/10.1085/jgp.201010542

Zalk, R., O.B. Clarke, A. des Georges, R.A. Grassucci, S. Reiken, F. Mancia, W.A. Hendrickson, J. Frank, and A.R. Marks. 2015. Structure of a mammalian ryanodine receptor. *Nature*. 517:44–49. https://doi.org/10.1038/nature13950

Zhou, J., G. Brum, A. González, B.S. Launikonis, M.D. Stern, and E. Ríos. 2005. Concerted vs. Sequential. Two activation patterns of Vast arrays of intracellular Ca^{2+} channels in muscle. *J. Gen. Physiol.* 126:301–309. https://doi.org/10.1085/jgp.200509353